The Pennsylvania State University

The Graduate School

STUDY OF LASER-INDUCED GRAPHENE BASED FLEXIBLE HUMIDITY SENSOR

A Thesis in

Engineering Science and Mechanics

by

Zhaozheng Yu

Submitted in Partial Fulfillment
of the Requirements
for the Degree of

Master of Science

December 2019

The thesis of Zhaozheng Yu was reviewed and approved* by the following:

Huanyu Cheng
Assistant Professor of Engineering Science and Mechanics
Research adviser

Elzbieta Sikora
Associate Teaching Professor and Graduate Programs Coordinator

Jian Hsu
Professor of Engineering Science & Mechanics

Judith Todd
Department Head of ESM
P.B. Breneman Chair
Professor of Engineering Science and Mechanics

Abstract

Capacitive humidity sensors based on laser-induced graphene (LIG) were fabricated by using the CO_2 laser to scribe on the commercial polyimide thin film (thickness = 50μm). The laser-ablated region of the polyimide turns into a porous structure with carbon as the main composition. Raman spectra and scanning electron microscope were used to characterize the LIG's chemical and morphology. Patterning LIG into the interdigitated electrode (IDE) to serve as both the electrode and sensing materials was achieved in one step. The proposed flexible humidity sensor demonstrates the sensitivity of 10% and response/recovery time of 109s/13.5s, respectively. In general, a promising humidity sensor with improved response/recovery time and good sensitivity can be fabricated in an easy, fast, and low-cost manner.

Table of contents

LIST OF FIGURES

LIST OF TABLES

Acknowledgments

I want to thank everyone who guided me through this project up to this point. My research advisor, Dr. Cheng is an excellent professor. His advice and suggestions lead me to the completion of this project. Graduate student, Ning Yi, and Jia Zhu, who guided me to test the sample and provided a lot of help throughout the project. Also, I would like to thank everyone in our laboratory for teaching me the usage of all the experimental equipment.

Introduction

1.1 Sensor

Since the first industrial revolution, mechanization changes the entire society and improve productivity. Nowadays, most of the people on longer suffer from the lack of food and water. Humanity never stops to develop science and technology, and they start to look for better ways to improve the quality of life. Along with the technology developed, humans invented the computer and the internet, and the way people exchange information changes. In the information era, the concept of the global village has glowing because of the information exchanges extremely fast. Now, human focus develops sensors to extend their perception; different types of sensors have widely applied in people's life and works[1]. A sensor is a device that can measure the specific property, such as pressure, temperature, humidity, or position, and send feedback to other devices to process the information. An ideal sensor has two features: the measurement of the sensor is only affected by the measuring factor and itself does not affect the measuring factor.[2]

1.1.1 Humidity sensor

Humidity control is essential for various fields of human activity including industrial production[3], food storage[4], virus transmission control[5], and agricultural production[6], etc. The development of humidity sensors enabled people to monitor the humidity change faster and more sensitivity. The traditional humidity sensor, psychrometer, was discovered in the early 18th century. Unfortunately, the measurement error of the psychrometer can reach more

than 7%, possibly due to the turbulence of airflow.[7] Recent decades witnessed the fast development of commercially available electronic humidity sensor with improved accuracy of 2%-3%.[8] Lithium chloride, polymer film, and porous ceramic-based humidity sensors are the most represented ones.[9] Researchers are investigating new materials with superior properties to improve the sensitivity, response/recovery rate, and the humidity range of humidity sensors. It is found that materials with nanostructures are of interest for humidity monitoring due to its dramatic increase of specific surface area can bring exceptional enhancement in humidity sensing.

Humidity sensors can measure and report the relative humidity (RH) in the air, so they are often integrated with home heating, ventilating, and air conditioning systems. Specifically, some patients have to stay in the room with specific relative humidity so humidity monitoring is vital for them. Also, some laboratory work has to be conducted in specific relative humidity, such as determination of influenza virus transmission under different relative humidity. This research shows the influenza virus is dependent on relative humidity, the stability of viral to be maximal at 20%-40% RH, and minimal at 50% RH.[5] Other than the medical instruments, many industrial areas also require humidity control to improve product quality, yield, and cost.[8] For example, different pharmaceutical manufacturing needs to be done at specific humidity levels. Higher or lower RH levels could affect surface finish, material stickiness to the stamping machine, and other problems.[10] Also, humidity control is closely related to food storage, such as sugar storage requires RH from 20% to 35%.[4]

There three basic types of humidity sensor in research and commercial products:

1.1.1.1 Capacitive humidity sensor

The capacitive humidity sensor measures relative humidity by tracking the capacitance change of the capacitor consisting of a dielectric material and a pair of electrodes. The capacitive sensor uses dielectric material with low dielectric constant (typically ranging from 2 to 15).[11] The dielectric constant (also known as relative permittivity) of water vapor is about 80 under room temperature; which is larger than the dielectric constant of the dielectric material. Therefore, when the water vapor absorbed by the dielectric material, it leads to an increase in the capacitance of the capacitor.[12, 13] This type of humidity sensor is widely used because it can measure the range of relative humidity from 0% to 100%. There are two different structures of capacitive-type humidity sensors: parallel plate electrode structure and interdigitated electrode structure. The capacitance of the parallel plate electrode capacitive humidity sensor can be expressed as:

$$\mathrm{C} = \varepsilon_r \times \varepsilon_0 \times \left(\frac{A}{d}\right) \tag{1.1}$$

Where A is the effective area of two parallel plates, d is the distance between two electrodes, ε_r is the dielectric permittivity as a function of the relative humidity, and ε_0 is the dielectric permittivity of free space. The equation for the capacitance of the interdigitated electrode humidity sensor is similar to equation (1.1) where d is the distance between two fingers, and A is equal to the length times the depth of the fingers.[13] Polymer film, ceramic, and metal oxide are commonly used sensing materials for capacitive type humidity sensor. Noble metals such as silver (Ag), gold (Au), and copper (Cu) are the most frequently used materials for the electrode.[14-17] Figure 1 shows the structure of two typical capacitive

humidity sensors.

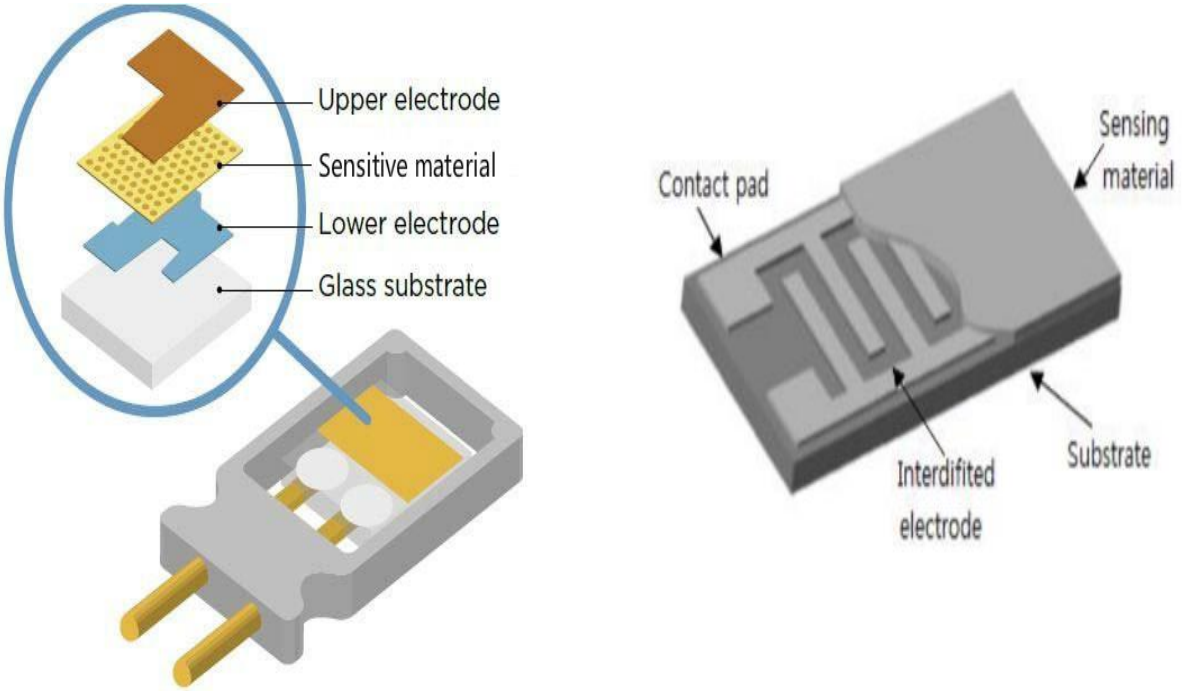

Figure 1. The left figure shows a typical structure of a parallel plate electrode type humidity sensor. The right figure shows the typical structure of an interdigitated electrode type humidity sensor.[14][18]

1.1.1.2 Resistive humidity sensor

The resistive humidity sensor measures the change in electrical resistance of the sensing material. At a given humidity condition, the adsorption and desorption of water molecules to the sensing materials will reach an equilibrium state gradually. The charge transfer between water molecules and the sensing materials can change the carrier density of the sensing material and affect its resistance. Different types of sensing materials such as metal oxide, carbon-based nanomaterials, and polymers have been proposed for humidity monitoring applications. Representative materials include anodic aluminum oxide (AAO)[16], multiwalled carbon nanotube (MWCNT)[19], and polyimide[15]. The resistive type humidity sensor normally takes the form of an interdigitated electrode, where sensing materials are drop cast on top so that a parallel circuit is formed to reduce the resistance to the measurable range significantly.

Upon water molecule adsorption to the surface of sensing material, the resistance can either increase or decrease, depending on the carrier type (electrons or holes) of the material. The structure of the resistive humidity sensor is shown below:

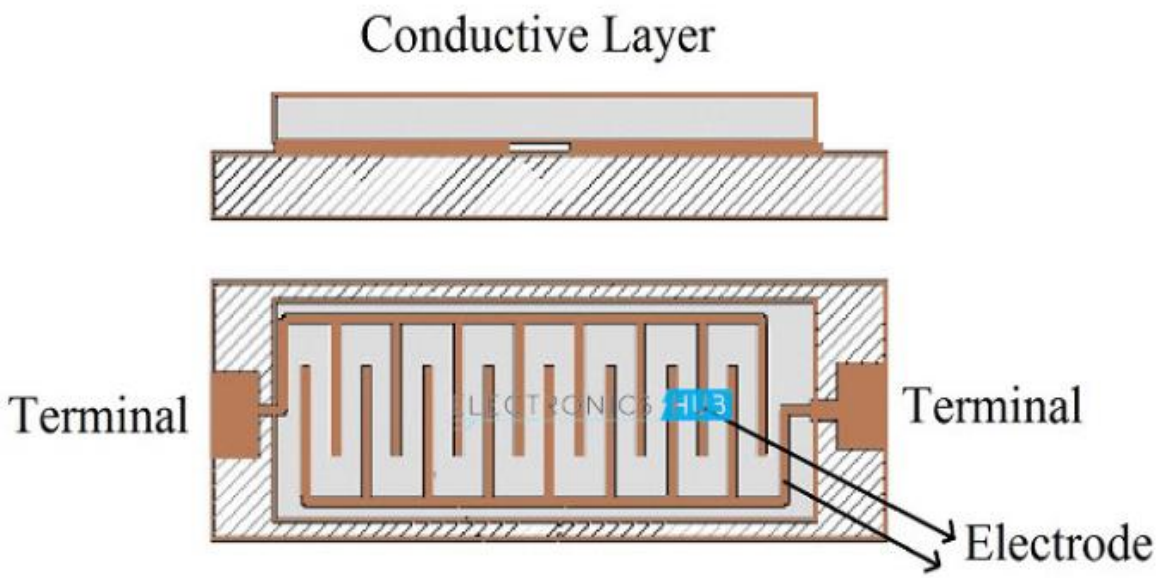

Figure 2. Structure of an interdigitated electrode resistive humidity sensor.[20]

The resistive humidity sensor is also based on the interdigitated electrode. The interdigitated electrode patterns are used to increase the contact area. When the conductive layer (sensing material) absorbs water vapor from the surrounding air, the resistivity between the electrodes changes. Salt, solid polyelectrolytes, and conductive polymers are commonly used for the conductive layer.[20]

1.1.1.3 Thermal humidity sensor

The thermal humidity sensor is quite different from the other two sensors. It is a commonly used sensor to measure absolute humidity (AH). It is a combination of two thermistors, while one sensor is in contact with dry nitrogen, the other encased with the surrounding air. The resistance of the two thermistors was measured, and the difference between those two values

can be used to determine the absolute humidity.[20]

Plenty of nanomaterials such as Multi-Wall Carbon Nanotubes[19], Polyimide[15], anodic aluminum oxide[16], and MoS_2/SnO_2[17] have been employed to fabricate humidity-sensing devices. Those materials all show the great result as humidity sensor in the different range of relative humidity. The laser-induced graphene has 3D porous structure and high electrical conductivity, which is a potential material for making a humidity sensor. The 3D structure and porous gives the material a larger surface area and better hygroscopic property, and the high electrical conductivity may lead to the high sensitivity of humidity.

1.1.2 Main performance parameters

The humidity sensor is a device that can detector humidity and send electrical signal output to others to express different levels of humidity.[16, 23]

1.1.2.1 Relative humidity range

This parameter shows the maximum range of relative humidity that a humidity sensor can measure. The lager the humidity range, the greater the value of its practical application. An ideal range of a humidity sensor is 0%RH~100%RH.

1.1.2.1 The response curve of relative humidity

Different humidity sensors have different humidity characteristics; for example, the impedance of a resistance-type humidity sensor is change along with the changing relative humidity. The curve shows this relationship between two values is called the response curve of

relative humidity. The response curve of relative humidity for an ideal humidity sensor should be continued over its relative humidity range, which means the linear the better.

1.1.2.3 Sensitivity

Sensitivity is the slope of the response curve of relative humidity in each relative humidity level. It shows the degree of change humidity characteristic along with changing relative humidity in the environment.

1.1.2.4 Response and recovery time

Response and recovery time shows the changing speed of the humidity characteristic, along with changing relative humidity. Response time is the time that humidity characteristic stops changing when a humidity sensor moved from a low relative humidity environment to a high relative humidity environment. Recovery time is the time that humidity characteristic stops changing when a humidity sensor moved from a high relative humidity environment to a low relative humidity environment. The lower the response and recovery time, the better the humidity sensor is. For an ideal humidity sensor, the value of humidity characteristic should return to the same value when the sensor return to the same relative humidity environment.

1.2 Humidity and measurement

Humidity is a value that shows the concentration of water vapor percentage in the surrounding environment. These are three basic forms of showing humidity:

1.2.1 Absolute humidity

Absolute humidity (AH) shows the ratio of the mass of water vapor (m_{H_2O}) over the volume of air (V_{air}) at the given temperature. The equation of absolute humidity can be expressed as:

$$\text{AH} = \frac{m_{H_2O}}{V_{air}} = \text{g}/m^3 \tag{1.2}$$

The maximum absolute humidity appears at saturated humidity.

1.2.2 Relative humidity

The relative humidity (RH) is the ratio of the partial pressure of water vapor (P_{water_vapor}) to the equilibrium vapor pressure of water (P_{sat_vapor}) at a specific temperature. It depends on the water content in the air and the temperature:

$$\text{RH\%} = 100\frac{P_{water\_vapor}}{P_{sat\_vapor}} \tag{1.3}$$

The relative humidity is an important factor in human thermal comfort. The study shows that the recommended range of indoor relative humidity is 30-60% under room temperature.

The applications of the humidity sensor are open and wide. This device is often part of home heating, ventilating, and air conditioning systems. Some illness patient has to stay in the room with specific humidity which counts on the humidity sensor. Also, a lot of experiments require specific relative humidity in the environment. For example, to determine influenza virus transmission under different relative humidity.[11]

1.2.3 Specific humidity

Specific humidity (SH) is the total mass of water vapor (m_{H_2O}) present in a given mass of

air (m_{air}). The specific humidity of a sealed air does not change with the temperature as long as no condensation or evaporation appears. Specific humidity can be expressed as:

$$\mathrm{SH\%} = \ 100\frac{m_{H_2O}}{m_{air}} \tag{1.4}$$

Humidity plays an important role in our medical, manufacture industry, agriculture industry, and daily life. Those three primary measurements of humidity are widely used in different fields.

1.3 Graphene and Laser-Induced Graphene (LIG)

Nowadays, scientists are looking for new materials that have improved properties compared with conventional materials, either lighter, stronger, or more conductive. People tend to make materials more complexed, such as alloys.

In such a trend, Graphene isolated and characterized in 2004 by Andre Geim and Konstantin Novoselov at the University of Manchester.[23, 24] Scientists have theorized about Graphene as far back as the early 20th century. Graphene, the latest discovered carbon nanostructure, is an allotrope of carbon in the form of a two-dimensional hexagon form in which one atom forms each vertex.[25]

Graphene often refers to two-dimensional (2D) forms of carbon atoms arranged in a hexagonal lattice. Graphene can be prepared by several methods, including wet-chemical approaches and chemical vapor deposition (CVD). However, no method can prepare 2D graphene beyond a small size yet.[30, 31] There are differences between graphene and graphite. Graphene is defined as one atom thick (~0.34 nm in thickness), but in many research and applications, the graphene has been designed into three-dimensional (3D) porous structure. This structure, the graphene can maintain its unique mechanical properties and high electrical

conductivity and gain a larger surface area. The microstructure of Graphene is shown in Figure 3.

Graphene has many extraordinary physical properties. Graphene is 100 times stronger than steel in the same thickness with lower density. It is also a heat and electric conductor with electron mobility of 15000 $cm^2V^{-1}s^{-1}$.[26] According to the reported result, 50 square meter Graphene can support a 5kg weight speed up to the first cosmic velocity within 20 minutes.[26]

Base on graphene's physical properties, no doubt, it will be used to making integrated circuits and chips. Although Graphene is used in multiple different fields, it still has great potential. Many research groups studied Graphene-based humidity. Bi et al. have used graphene oxide (G-O) film as humidity sensitivity material to make an ultrahigh sensitivity humidity sensor.[31] Their result shows a sensitivity up to 37800% at 1kHz frequency, the fast response time (10.5s), great long-term stability. But the capacitance response to RH of this G-O film-based capacitive humidity sensor is a non-linear curve, and it also shows slow recovery time (41s). Chen et al. manufactured a bilayer graphene humidity sensor with response time in the millisecond interval. The manufacturing technology of this humidity sensor is quite difficult. In the letter, the bilayer graphene was synthesized on a copper foil by chemical vapor deposition (CVD), then transfer to the glass substrate. The result also shows the highest sensitivity of this bilayer graphene humidity is only 18.1%.[33] The supercapacitor is another highly anticipated field for graphene use because graphene has a very big percentage of surface

versus mass.[26]

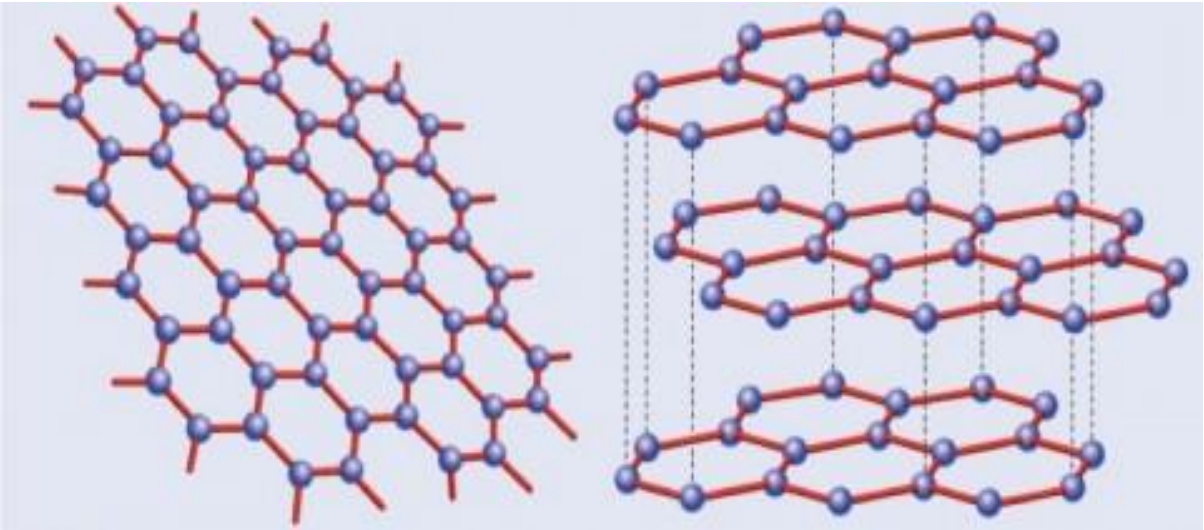

Figure 3. The schematic of the atomic structure of monolayer graphene ((left)) and LIG (right).[29]

Although graphene is a special material, one of the main reasons that this material has not yet been widely used in commercial products is it is high cost and difficult to mass-produce self-designed conductive graphene patterns. Lin et al. found a new way to produce patterned graphene by laser cutting thin polyimide (PI) film.[23] The resulting material is called laser-induced graphene (LIG). LIG has a similar structure as graphene, except it has multilayers. This property shows a one-step laser scribing on commercial PI film in the air from 3D graphene layers. In this paper, we demonstrate the LIG can be used to create a humidity sensor based on its porous structure because the structure proves a large contact area with the surrounding air. Moreover, the LIG based humidity sensor has very high sensitivity, great response and recover speed, easily manufactured, and stretchability.

The linear response, response/recovery time, and stability in large temperature range are the biggest challenges that current humidity sensors facing, also the cost and complex manufacture are the most common challenges.[21] In this thesis, I will address the properties of LIG based capacitive interdigitated electrode type humidity sensor. LIG can be

manufactured by a one-step laser cut, which is easier to make an interdigitated electrode humidity sensor. This one-step laser cutting can lead to easy and low-cost manufacture. The 3D porous structure of LIG material provides a large contact area between material and air, which may lead to high sensitivity and fast response/recovery speed.[21]

Design and preparation of a capacitive humidity sensor

2.1 Design of humidity sensor

A widely employed configuration of a capacitive humidity sensor is a parallel capacitor with two electrodes sandwiching the dielectric sensing material. However, such configuration limits the adsorption and migration of water molecules to the dielectric only on the edge of the capacitor. Here in this study, an interdigitated electrodes patter was proposed where the Archimedean spiral structure of the electrode is functioning the same as the electrode for a conventional parallel capacitor. With the dielectric materials and electrode exposed to air, diffusion and absorption of water molecules are therefore facilitated.

2.1.1 Principle of the capacitive humidity sensor

The capacitive humidity sensor comprised of a hygroscopic dielectric material placed between a pair of electrodes. When the humidity level changes, the dielectric constant of the hygroscopic dielectric material changes. As a result, the capacitance of the humidity sensor changes.[16, 34] The Interdigitated electrode structure is commonly used for capacitive because it provides a highly effective area, which can lead to large capacitance in a small sample size.[35]

1. Interdigitated Electrodes

The interdigitated electrode, which is depicted in Figure 4, is the most common design for gas or humidity sensors, it has many advantages. IDEs achieve high capacitance in minimized overall size. The capacitance of the ideal interdigitated electrode can be expressed as the

following equation (2.1):

$$C = \varepsilon_r \times \varepsilon_0 \times (\frac{A}{s}) \quad (2.1)$$

where A is the effective area. s is the distance between two adjacent 'fingers'. If the thickness of the electrode w is very small compare to the 'finger' length L, then $A = L \times (N-1) \times d$. d represents the depth of the electrode, and N is the number of 'fingers'. The 'fingers' of the IDE structure hence increase the overall effective area of the sensor and leads to an increase in the capacitance of the device. By increase overall capacitance, we reduce the noise of the material and increase the sensitivity of the sensor. It is easier to manufacture an interdigitated electrode type LIG humidity sensor rather than the parallel plate type due to the laser cut process.

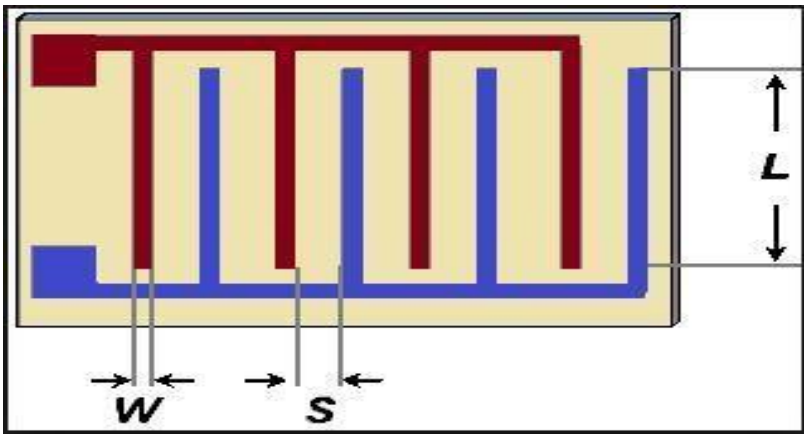

Figure 4. The geometry of the interdigitated electrode in 2D.[36]

2. Archimedean Spiral

The Archimedean spiral, or arithmetic spiral, is a spiral named after Greek mathematician Archimedes (3rd-century BC). This spiral can be drawn by a point that rotates with constant angular velocity. It can be described by the equation (in polar coordinates r,θ)[37]:

$$r = a + b\theta \quad (2.2)$$

where a and b are real numbers. The parameter 'a' can turn the spiral, while b controls the distance between each turn. By using two paralleled Archimedean spirals, an interesting capacitor structure can be created, as shown in Figure 5. The capacitance of the Archimedean spiral is similar to the normal IDEs, expect the effective area $A = L \times d$. Where L is approximately equal to the total length of two spirals, and d is the depth of the Archimedean spiral. The Archimedean spiral is equally distributed and paralleled to each other. This unique structure provides a larger effective area than IDEs with a similar overall size, which leads to higher capacitance. The Archimedean Spiral is formed by two curved lines. This pattern could have better stretchability than normal interdigitated electrodes. Normal interdigitated electrodes were formed by straight lines. When the sample been stretched, the straight line is earlier to have a fracture because the curved line has more room to deformation along with the stretch. Therefore, the Archimedean spiral would be a great structure for our humidity sensor.

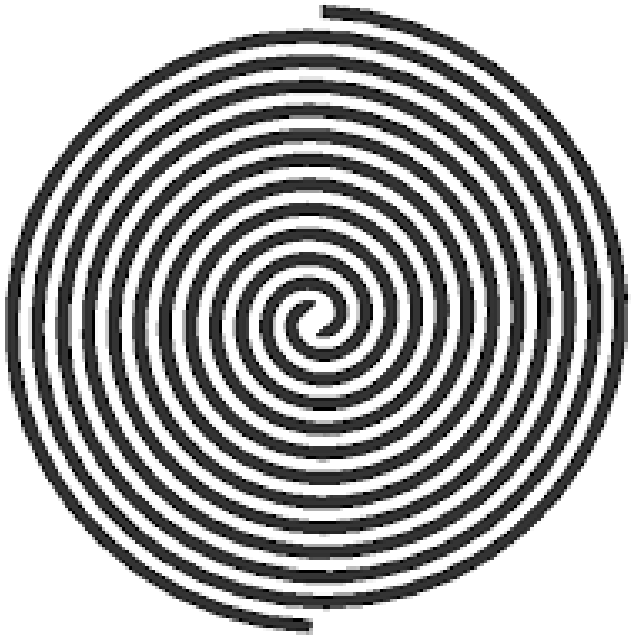

Figure 5. The geometry of the Archimedean spiral capacitor in 2D.

2.1.2 The relationship between the dielectric constant of air and relative humidity

Consider the moist air is an ideal gas that constitutes by dry air and water vapor. Clausius-Mossotti equation can express the dielectric constant (ε_r) of a material in terms of the atomic polarizability, α, of the material's constituent atoms[65]:

$$\frac{\varepsilon_r - 1}{\varepsilon_r + 2} = \frac{N\alpha}{3\varepsilon_0} \tag{2.3}$$

where ε_r is the dielectric constant of the air, ε_0 is the permittivity of free space, N is the number the molecules, and α is the molecular polarizability (C·m2/V). For air $N_{air} = N_{dry\_air} + N_{water\_vapor}$. For polar gas: $\alpha = \alpha_e + \frac{\mu^2{}_0}{3kT}$, where α_e is displacement polarizability, and $\frac{\mu^2{}_0}{3kT}$ is the steering polarizability. Apply those to equation (2.3):

$$\frac{\varepsilon_r - 1}{\varepsilon_r + 2} = \frac{N_{dry\_air}}{3\varepsilon_0}\alpha_{e1} + \frac{N_{water\_vapor}}{3\varepsilon_0}(\alpha_{e2} + \frac{\mu^2{}_0}{3kT}) \tag{2.4}$$

Gibbs-Dalton's law of partial pressures (2.5) shows[66]:

$$P_{air} = P_{dry\_air} + P_{water\_vapor} \tag{2.5}$$

where P_{air} is atmospheric pressure, P_{dry_air} is the partial pressure of dry air in the moist air, P_{water_vapor} is the partial pressure of water vapor in the moist air. $P = NkT$, Therefore $P_{air} = (N_{dry\_air} + N_{water\_vapor})kT$

$$N_{dry\_air} = \frac{P_{air}}{kT} - N_{water\_vapor} \tag{2.6}$$

Substitute equation (2.6) into equation (2.4)

$$\varepsilon_r = 1 + \frac{P_{air}}{\varepsilon_0 kT}\alpha_{e1} + \frac{N_{water\_vpor}}{\varepsilon_0}(\alpha_{e2} + \frac{\mu^2{}_0}{3kT} - \alpha_{e1}) \tag{2.7}$$

From the defamation of the relative humidity

$$\text{RH\%} = 100\frac{P_{water\_vapor}}{P_{sat\_vapor}} \tag{2.8}$$

where P_{water_vapor} is the pressure of water vapor, P_{sat_vapor} is the pressure of saturated

water vapor at the same temperature. Therefore:

$$N_{water\_vapor} = \frac{RH \times P_{sat\_vapor}}{kT} \tag{2.9}$$

Using the Antoine equation[38]:

$$lnP_{sat\_vapor} = A - \frac{B}{C + T} \tag{2.10}$$

where T is temperature, $A, B, and\ C$ are component-specific constant. $A = 23.7836$, $B = 3782.89$,

From Clausius-Mossotti equation (2.7), combined with Dalton's law of partial pressures (2.3) and Antoine equation (2.10) we can derive an equation from expressing the relationship between dielectric, temperature, atmospheric pressure, and humidity.

$$\varepsilon_r = 1 + 1.67810 \times 10^{-6} \frac{P_{air}}{T} - 2.3415 \times 10^{-9} \frac{RH \times P_{sat\_vapor}}{T} + 7.4212 \times 10^{-5} \frac{RH \times P_{sat\_vapor}}{T^2} \tag{2.11}$$

Apply this relation into Matlab, assume the ideal situation (T = 393K, 1 standard atmospheric pressure, the dielectric constant of dry air = 1.00058). The value of the dielectric constant increased by ~0.0002 when the relative humidity changes from 0% to 100%. Therefore the effect from the dielectric constant of air in the humidity test is negligible.[39]

2.1.3 The relationship between temperature and relative humidity

Temperature and relative humidity are two important factors that indicate the amount of moisture in the air. The relationship between these two factors is extremely complexed that requires a large number of equations and calculations. Mark *et al.* found a simple conversion of the relationship between temperature and relative humidity. The relationship can be expressed as equation (2.12)[40]:

$$RH\% \approx 100 - 5(T - T_d) \tag{2.12}$$

where T is the temperature, and T_d is the dew-point temperature. Dew-point temperature According to this equation, the relative humidity decrease by 5% for every 1°C increase in temperature at the same dew-point temperature. Therefore temperature control is necessary during the humidity test. Our experiment was placed in a temperature-controlled laboratory that maintains the temperature at 23°C.

2.2 Humidity sensor fabrication

2.2.1 Prepare designed LIG pattern on PI file

Polyimide thin film (thickness = 50μm) is first bonded to a glass slide through a water-soluble tape/double-sided tape double-layer structure. The water-soluble tape serves as a sacrificial layer that will release the polyimide film upon dissolution in water. The double-sided tape was used to bond the polyimide tightly onto the glass slides so that a flat surface is ensured. Figure 6, 7 shows the flow chart of the LIG humidity sensor fabrication. The LIG is formed by using a CO_2 laser cutting machine (Universal) with a speed of 16% and a power of 10% in raster mode. A computer-assisted design (CAD) tool was used to design the pattern. During laser ablation, the photonic energy of the laser was converted into thermal energy and thus burned the polyimide locally within the spot size of the laser. Since the polyimide possesses the highest glass transition temperature among polymers, it is believed that the local temperature inside the laser spot should be higher than 400°C. The porosity of the LIG is also found to be proportional to the laser power. Immersing the multilayer structure into water dissolves the water-soluble tape and thus release the polyimide thin film and the LIG residing on it. Raman spectra (Figure 8) was used to characterize the chemical information of LIG. Raman spectra of LIG exhibited three characteristic peaks, the D peak at ~1350 cm^{-1}, the G peak at ~1580 cm^{-1}, and the 2D peak at ~2700 cm^{-1}. The existence of the 2D peak suggests the formation of graphene. The small D/G ratio from the Raman spectra indicates a high quality of graphene. The ratio of the 2D/G is ~0.48 that represents a multi-layer graphene structure of LIG.[41, 42]

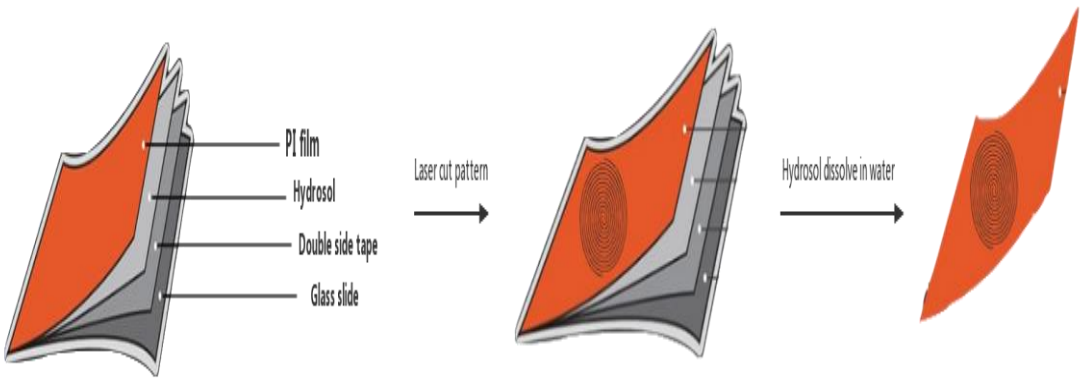

Figure 6. Schematic illustration for remove LIG sample with PI film from the glass slide.

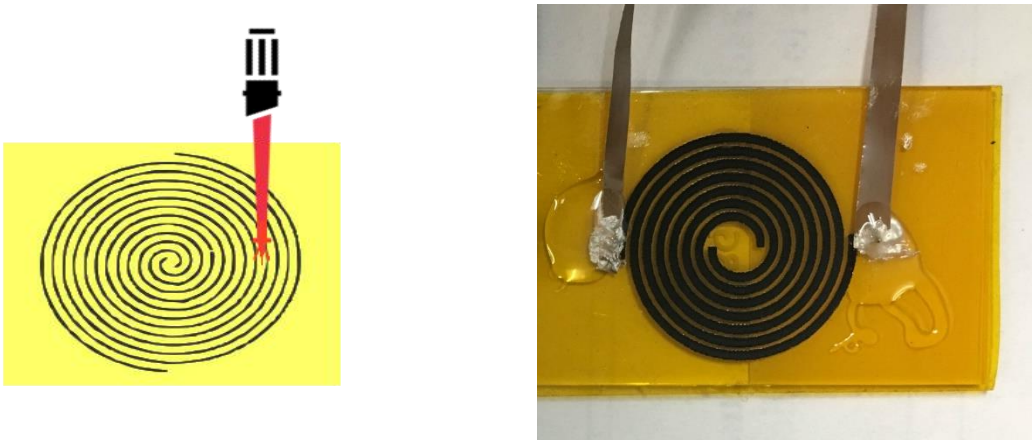

Figure 7. LIG formation under ambient conditions. The left figure shows a schematic of the synthesis process of LIG from PI film. The right figure shows an actual LIG pattern on PI film.

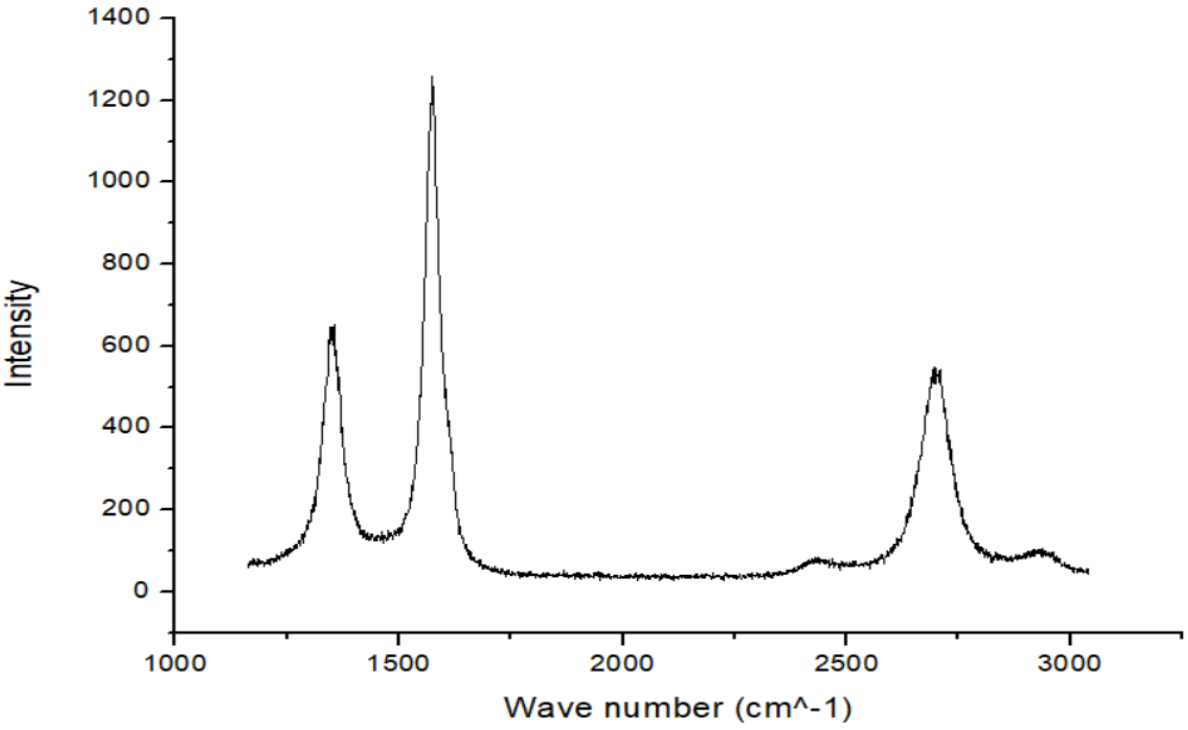

Figure 8. Raman spectra of LIG.

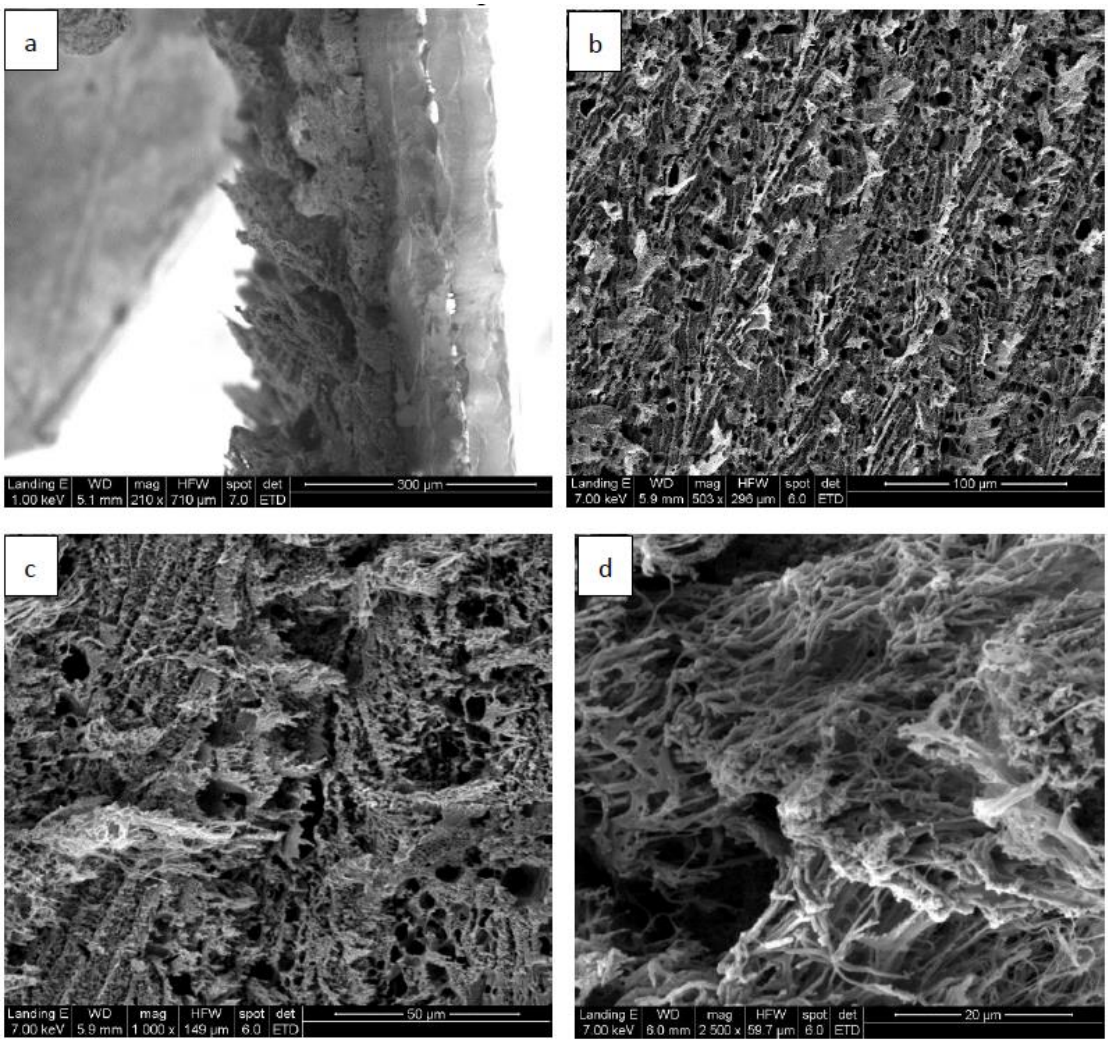

Figure 9. LIG structures under SEM. (a) SEM image with a 210X magnification of the cross-section of LIG structure. The thickness of LIG is about 30µm. (b) SEM image with a 503X magnification of LIG structure surface. (c) SEM image with 1000X magnification of LIG structure surface. (d) SEM image with a 10000X magnification of LIG structure surface.

The SEM image of our LIG sample, shown in Figure 9, shows the thickness of it is approximately 30µm. The image shows the LIG forms a fibers-like structure with diameters within several microns and micropores in between clusters of carbon fibers. This type of structure can enlarge the surface area of the carbon materials to provide additional sites for the interaction with water vapor. At the same time, the highly porous structure can facilitate the penetration of water vapor into the LIG. This unique structure means the LIG has strong hygroscopic potential, which could lead to high sensitivity and short response/recovery time

response to relative humidity.

The capacitance of the Archimedean spiral LIG humidity sensor can be expressed as equation (2.13):

$$C(\emptyset) = \varepsilon(\emptyset) \times \varepsilon_0 \times (\frac{A}{s}) \quad (2.13)$$

where $\varepsilon(\emptyset)$ is the permittivity of the sensing material (LIG) as function of the volume fraction of condensed water vapor $\emptyset$, A is the effective area, and s is the distance between paralleled Archimedean spirals. $\emptyset$ can range between 0 and 1. The sensitivity (S) can be defined by equation (2.14)[43]:

$$S = \frac{C(\varepsilon) - C(0)}{C(0)} \quad (2.14)$$

where $C(0)$ is the smallest capacitance of the humidity sensor for $\emptyset = 0$, which is in the dry air environment. $C(\varepsilon)$ is the largest capacitance of the humidity sensor, which is found for $\emptyset = \varepsilon$, i.e., the porosity of LIG. The relationship of volume fraction $\emptyset$ and porosity ε can be expressed with:

$$\emptyset = \varepsilon(\frac{P_{water\_vapor}}{P_{sat\_vapor}})^n \quad (2.15)$$

where ε is porosity, and n is a parameter dependent on pore radius distribution. This equation explains the relationship between pore structure and relative humidity.

2.2.2 Transfer LIG humidity sensor onto the flexible substrate

As we discussed in the previous chapters, the Archimedean spiral interdigitated electrode is designed for the wearable humidity sensor. It has to be on the flexible substrate to test its stretchability. The polyimide (PI) film has high tensile strength (~200MPa), which is very hard to be stretched. The tensile strength of the substrate equal to or less than human skin (~27MPa)

will make the wearable sensor more comfort for users.[44] Therefore, transfer the LIG pattern from PI film to a flexible substrate is necessary.

Polydimethylsiloxane (PDMS) is a commonly used flexible substrate in lots of research. It is widely used due to its easy fabrication, low cost, softness, optical transparency, moldability, low surface energy, and weak chemical reactivity. The traditional PDMS (SYLGARD-184) is very fragile. The yield of PDMS is only 40%.[45] It has good bendability but poor stretchability. Dragon Skin™ silicones are high-performance platinum cure liquid silicone compounds. Dragon Skin™ and PDMS are both silicon-based organic polymer. The tensile strength of Dragon Skin™ silicone is about 3MPa, and its elongation at break is 1000%, which satisfies the test requirement.

Uncured Dragon Skin™ silicone is a viscoelastic liquid. The mechanical properties have significant changes after curing. These properties make cured liquid silicone compounds very popular in the research laboratory because it can be easily molded to the desired shapes.

Transfer LIG structure from PI film onto Dragon Skin™ silicone substrate is a big challenge. LIG has a very fragile porous structure. Even little scratches could cause significant damage to the sample. Therefore the traditional way of using adhesive force to peel the sample off from the original substrate is not working in this case.

After several times of experiments and discuss with a cooperator (Zheng Yan from the Department of Mechanical and Aerospace Engineering, University of Missouri), we finally discovered a steady way to transfer the LIG pattern onto Dragon Skin™ silicone substrate.

After laser-cut LIG pattern on PI film, cover LIG pattern with Uncured Dragon Skin™ silicone mixture. Uncured Dragon Skin™ silicone mix with heptane in the ratio of 2:1. Uncured Dragon Skin™ silicone has high viscosity and fast curing speed. Mixing Uncured Dragon Skin™ silicone with heptane will decrease its viscosity, which helps to make a thin substrate and remove bubbles before it is completely cured. Decrease the viscosity also helps silicone liquid to have a close interface with LIG pores. Heptane is a volatile liquid, which will completely evaporate before Dragon Skin™ silicone is cured. A schematic flow chart of the transfer printing processes is depicted in Figure 10.

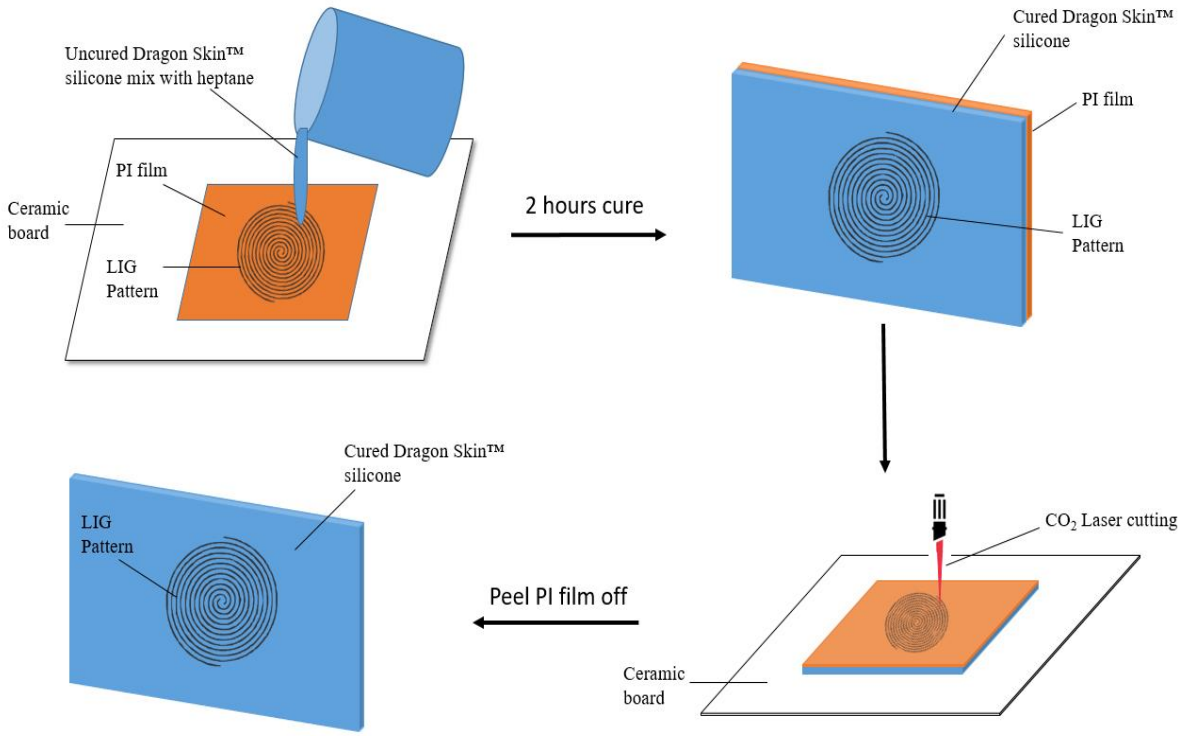

Figure 10. Flow chart for transfer LIG pattern onto Dragon Skin™ silicone substrate.

After Dragon Skin™ silicone complete cured, putting the sample on the ceramic board with silicone side facing down and using the CO_2 laser cut again to etching over the LIG pattern from the backside of the PI side. Laser beam generates a large amount of heat on a small area during the etching process, the coefficient of thermal expansion of PI film and LIG is different

($35.9x10^{-6}$ K^{-1} and $-7x10^{-6}$ K^{-1}).[46, 47] Therefore, the PI film will be separated from LIG and left it on the Dragon Skin™ silicone substrate.

Transfer printing of LIG onto the Dragon Skin™ silicone substrate will cause damage to the LIG structure. The difference between resistances of the LIG pattern before and after transfer print shows the level of damage. The test shows the capacitance of the LIG pattern before the transfer print is 8.637pF, the capacitance of LIG after transfer pattern is 8.25pF. The difference between transfer print before and after is less than 5%. This error is acceptable for now. Transfer printed LIG patterns on Dragon Skin™ silicone substrate is shown in Figure 11.

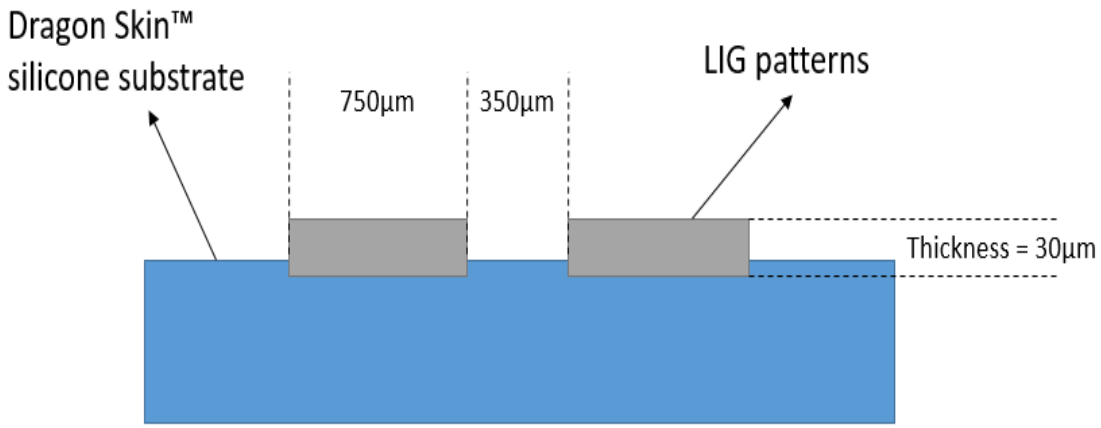

Figure 11. LIG patterns on Dragon Skin™ silicone substrate

Experimental setup

3.1 Relative Humidity control chamber

The saturated salt solution can be used to maintain particular values of relative humidity inside a sealed container.[48] This argument can be explained by Raoult's law.[49] As mentioned in the introduction part, the relative humidity can be calculated by the following equation (3.1):

$$\mathrm{RH\%} = 100\frac{P_{water\_vapor}}{P_{sat\_vapor}} \tag{3.1}$$

Moreover, the vapor pressure above the saturated salt solution is given by the equation below:

$$P_{water\_vapor} = P_{sat\_vapor} \cdot X_w = \ \mathrm{kg} \cdot m^{-1} \cdot s^{-2} \tag{3.2}$$

Where X_w is the mole fraction of water in the solution. Therefore the value of relative humidity is equal to the mole fraction of water in the solution when it reached an equilibrium condition. Mole fraction is defined as the number of moles of a constituent divided by the total number of moles of a solution. For example, a 1 liter of saturated sodium chloride solution is placed in a container. The density of saturated sodium chloride solution is 1.202 g/ml, and the maximum solubility of NaCl in water is 357 g/l at 25°C. The molar mass of water is 18.02 g/mol, and the sodium chloride is 58.44 g/mol. From those constant values, we can calculate the number of moles of water and sodium chloride in 1 liter of saturated sodium chloride solution. The number of moles of water $n_w = 46.89$ mol and the number of moles of sodium chloride $n_s = 6.11$ mol.

$$\mathrm{RH\%} = \ X_w \ = \frac{n_w}{n_w + 2 \cdot n_s} \times 100\% = \ 79.3\% \tag{3.3}$$

There is an assumption that NaCl, as a strong electrolyte, is completely dissociated in aqueous solution. Therefore the factor of 2 appears in the denominator of the equation. Based on the calculation, the ideal value of relative humidity at the equilibrium condition is 79.3%.

Some common saturated salt solution and the relative humidity at different temperatures when reaches the equilibrium condition is listed in Table 1. In the experiment, the sodium chloride solution was used based on our laboratory condition.

Saturated Salt Solution	Temperature (°C) (deg F)										
	0	5	10	15	20	25	30	35	40	50	60
	Relative humidity (%)										
Ammonium nitrate			75	70	67	64	60	53			
Ammonium sulphate	82	82	82	82	81	81	81	80	80	79	
Magnesium chloride	34	34	33	33	33	33	32	32	32	31	29
Magnesium nitrate	60	59	57	56	54	53	51	50	48	45	
Lithium chloride	11	11	11	11	11	11	11	11	11	11	11
Potassium sulphate	99	98	98	98	98	97	97	97	96	96	
Potassium nitrate	96	96	96	95	95	94	92	91	89	85	
Potassium chloride	89	88	87	86	85	84	84	83	82	81	80
Potassium acetate			23	23	23	23	22				
Potassium hydroxide		14	12	11	9	8	7	7	6	6	5
Sodium chloride	76	76	76	76	75	75	75	75	75	74	75
Sodium nitrite					65	64	63	62	61		
Sodium dichromate	61	59	57	57	55	54	53	51	50	49	47

Table 1: Some common saturated salt solution and the relative humidity at a given temperature.[50]

NaOH, $Na_2Cr_2O_7$, NaCl, KCl, and Na_2HPO_4 (22%, 54%, 75%, 85%, 90%RH) saturated salt solution were used for humidity control during the experiment. These five saturated salt solutions proved humidity range from 22% to 90%.

3.2 Measurement equipment setup

Capacitance and impedance of LIG pattern are the main factors that determine humidity sensitivity. Experiments were performed within a container chamber. An acrylic substrate is designed to place the sensor inside the container chamber alone with a saturated sodium chloride solution and a commercial humidity monitor (AcuRite 00613MB). The humidity monitor is used to indicate the relative humidity inside the chamber during the experiments. The LIG based humidity sensor is connected to the LCR meter (Keysight E4980A/AL Precision LCR Meter) for capacitance and impedance measurement at different frequencies. The relative humidity is varied over a range of 22%–90%, and experiments at each frequency were carried out at least three times. The schematic of the equipment is depicted in Figure 12.

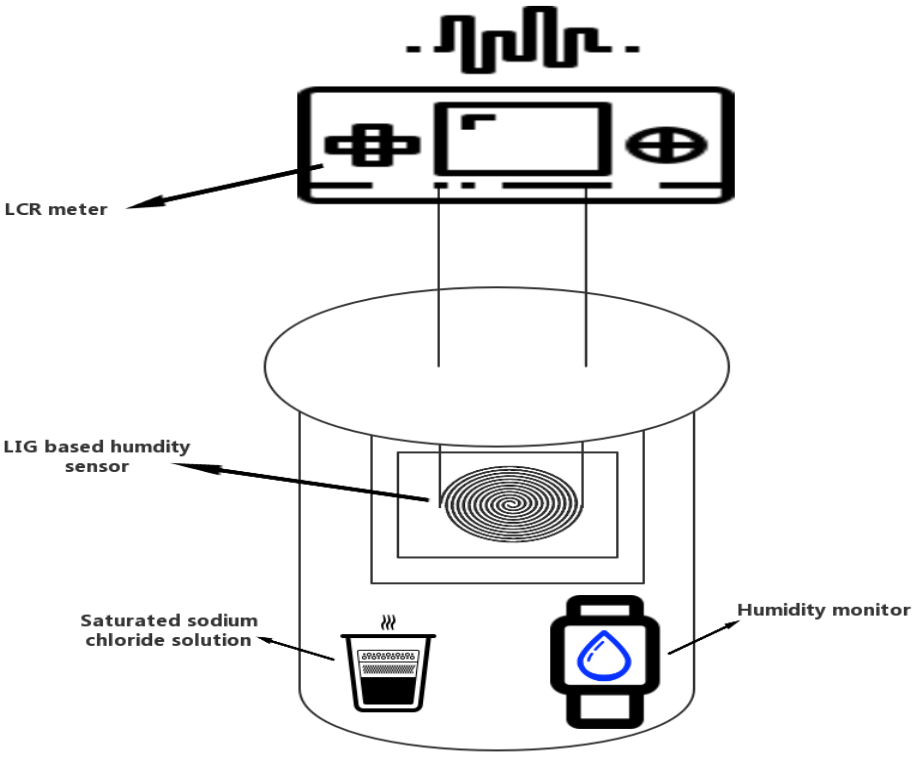

Figure 12. A schematic diagram of the equipment.

Keysight E4980A/AL Precision LCR Meter provides frequency range from 20Hz to

20MHz with 4-digit resolution in any range, but the accuracy of measurement would be rough when using the frequency near its limit. Therefore, we set the frequency at 100Hz, 1kHz, 10kHz, and 100kHz during the experiment to study how the frequency affects the sensitivity of our humidity sensor. During the experiment, the biggest problem I faced is it takes over five hours for the relative humidity to rise from 22% to 90%. The long experiment period greatly delayed the experiment's progress since we need to collect a huge amount of data for research analysis.

Results and Discussion

4.1 Sensitivity and Four Parameters Logistic Regression

Humidity sensitivity can show the value of the parameter (capacitance) of humidity sensor change when the relative humidity changes 1% in a relative humidity range. If the humidity sensor has high sensitivity, the changing value of capacitance will be relativity large. If the characteristic curve of the humidity sensor is linear, then the sensitivity does not change in different humidity ranges.

During the humidity test, the relative humidity was increased from 22% to 90% as different saturated salt solutions were placed inside the humidity chamber. Record 100 data points of capacitance at different frequencies when the RH inside the humidity chamber reached equilibrate condition. The response curves of the capacitance versus relative humidity at different frequencies of the LIG humidity sensor at 23°C is shown in Figure 13. The value of capacitance in each RH is the average value of 100 data points.

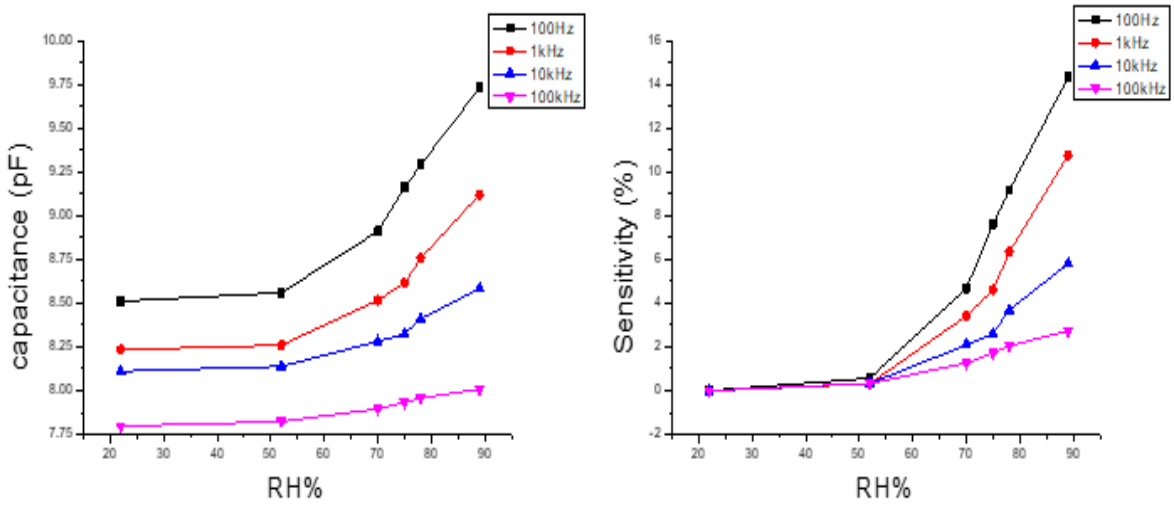

Figure 13. The left figure shows the response curves of the capacitance vs. relative humidity (RH) at different frequencies (100Hz, 1kHz, 10kHz, and 100kHz) of LIG humidity sensor. The right figure represents the sensitivity vs. RH at different frequencies of the LIG humidity sensor.

The result shows a non-linear response curve of the humidity sensor, and it is observed that capacitance decreases with increasing frequency. The sensitivity of the LIG humidity sensor increases with increasing RH and decreasing frequency.

The four parameters logistic (4PL) regression is a regression model that commonly used for curve-fitting analysis.[51] The equation for the 4PL model is:

$$\mathrm{y} = \mathrm{d} + \frac{a - d}{1 + (\frac{x}{c})^b} \tag{4.1}$$

where a is the minimum asymptote, b is Hill's slope of the curve, c is the point of inflection, and d is the maximum asymptote. Of course, x and y are independent and dependent variables, which are RH% and capacitance in the humidity test.[51, 52] Applied the experiment data onto the four parameters logistic regression, the relationship between the capacitance of LIG humidity sensor and relative humidity is shown in Figure 14. The coefficients of determination of those four curves are above 0.994. The coefficient of determination shows how better the curve fitting. It ranges from 0 to 1. If the coefficient of determination equal to 1, it means the dependent variable can be predicted without error.

LIG capacitive humidity sensor using LIG as the humidity sensing material. The relationship between relative permittivity of LIG ε_r and RH can be explained by Looyenga's empirical equation[53, 54]:

$$\varepsilon_r = [\gamma\left({\varepsilon_2}^{\frac{1}{3}} - {\varepsilon_1}^{\frac{1}{3}}\right) + {\varepsilon_1}^{\frac{1}{3}}]^3 \tag{4.2}$$

where ε_1 and ε_2 are representing temperature-dependent relative permittivity of LIG and water. γ represents the fractional volume of water absorbed by LIG. This equation can be used for solid material to absorb water vapor.

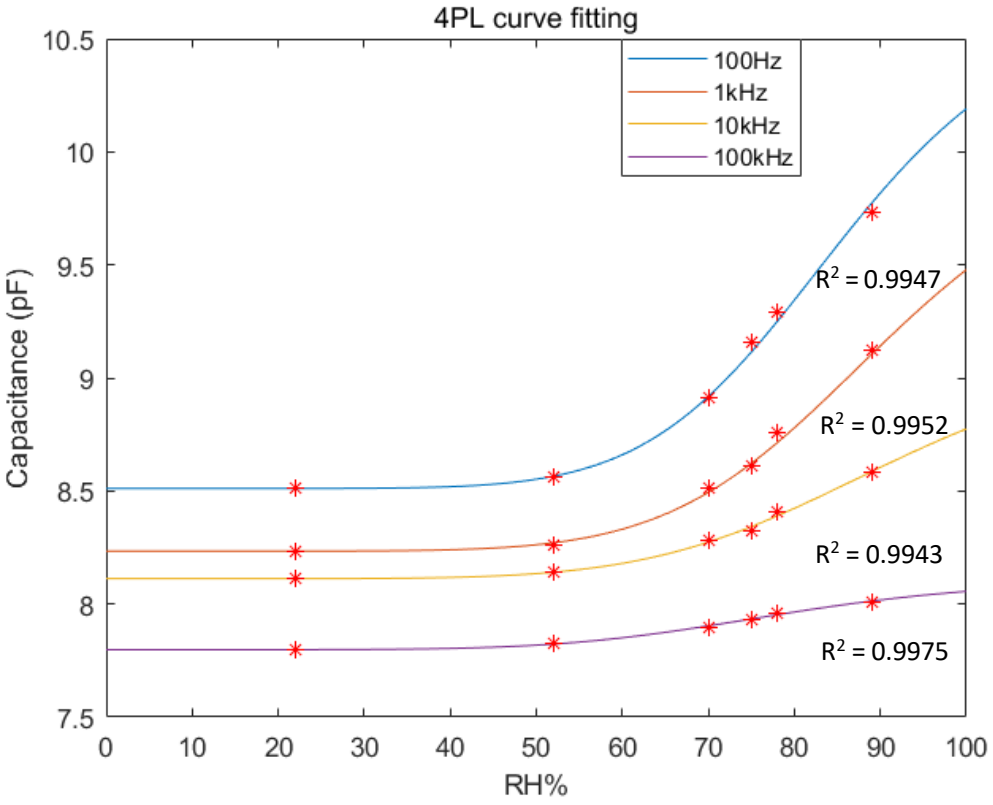

Figure 14. 4PL fitting curve figure for the LIG humidity sensor test result.

Shibata *et al.* present an equation to express the volume ratio of water vapor absorbed by solid:

$$\gamma = \gamma_m \emptyset_{(T)} x^{\Psi_{(T)}} \tag{4.3}$$

where γ_m is the maximum fractional volume of water absorbed by solid material at T_0, $T_0 = 298K$, $x = \frac{RH\%}{100}$, $\emptyset_{(T)}$ refers to the temperature dependence of the absorption coefficient, $\emptyset_{(T)} = 1 - \alpha_0(T - T_0)$, $\Psi_{(T)}$ refer to the temperature dependence of ε_2, and the catalytic effect. The Fickian model is applicable to the diffusion process. Substitute (4.3) into (4.2):

$$\varepsilon_r = [\gamma_m \emptyset_{(T)} x^{\Psi_{(T)}} \cdot \left(\varepsilon_2{}^{\frac{1}{3}} - \varepsilon_1{}^{\frac{1}{3}}\right) + \varepsilon_1{}^{\frac{1}{3}}]^3 \tag{4.4}$$

where γ_m, $\emptyset_{(T)}$, and $\Psi_{(T)}$ are temperature-dependent values. Those values maintain constant at the same temperature. The value of temperature dependence of the absorption coefficient $\emptyset_{(T)}$ is approximately 1 at 23°C (296.15K). The maximum sensitivity (S) of the capacitive

humidity sensor can be expressed as the following equation:

$$S = \frac{C(\emptyset)}{C_0} = \frac{\varepsilon(\emptyset) \times \varepsilon_0 \times (\frac{A}{s})}{\varepsilon(0) \times \varepsilon_0 \times (\frac{A}{s})} \quad (4.5)$$

where C_0 represents the capacitance of humidity sensor in dry air environment, and $C(\emptyset)$ represents the capacitance of humidity sensor in 100%RH environments, $\varepsilon(0)$ is the relative permittivity of sensing material at 0%RH, which is the relative permittivity of LIG. $\varepsilon(\emptyset)$ is the relative permittivity of sensing material at 100%RH. In an ideal situation, γ_m is equal to the porosity (Ɛ) of LIG. ε_1, ε_2 are constant values at 1kHz and 23°C. Therefore, the equation can be further derivation to:

$$S = \frac{\varepsilon(\emptyset)}{\varepsilon(0)} = \frac{[\text{Ɛ}1^{\Psi_{(T)}} \cdot \left(\varepsilon_2{}^{\frac{1}{3}} - \varepsilon_1{}^{\frac{1}{3}}\right) + \varepsilon_1{}^{\frac{1}{3}}]^3}{\varepsilon_1} \quad (4.6)$$

According to this equation, the sensitivity is depended on porosity (Ɛ) and the difference between relative permittivity of sensing material and water, and the linearity is depended on $\Psi_{(T)}$. If the $\Psi_{(T)} = 1$, the sensitivity of the humidity sensor should be perfectly linear. $\varepsilon_1 \sim 4$ and $\varepsilon_2 \sim 80.2$ at 23°C and 1kHz.[55] Using Matlab to do a regression model for fitting experimental data. The fitting curve and experimental data are shown in Figure 15. RH% was measured by a commercial humidity sensor. The coefficient of determination of the equation (4.6) is 0.9963, with $\Psi_{(T)} = 4.45$, and $\text{Ɛ} = 0.0271$. The maximum fractional volume (γ_m) of water absorbed by LIG is lower than expected, which indicates the porous structure of LIG has not fully utilized. The contamination of the LIG surface could cause a low fractional volume. The micro-level porous could be blocked by small dust in the air, which could affect

the ability to absorb water from the surrounding air.

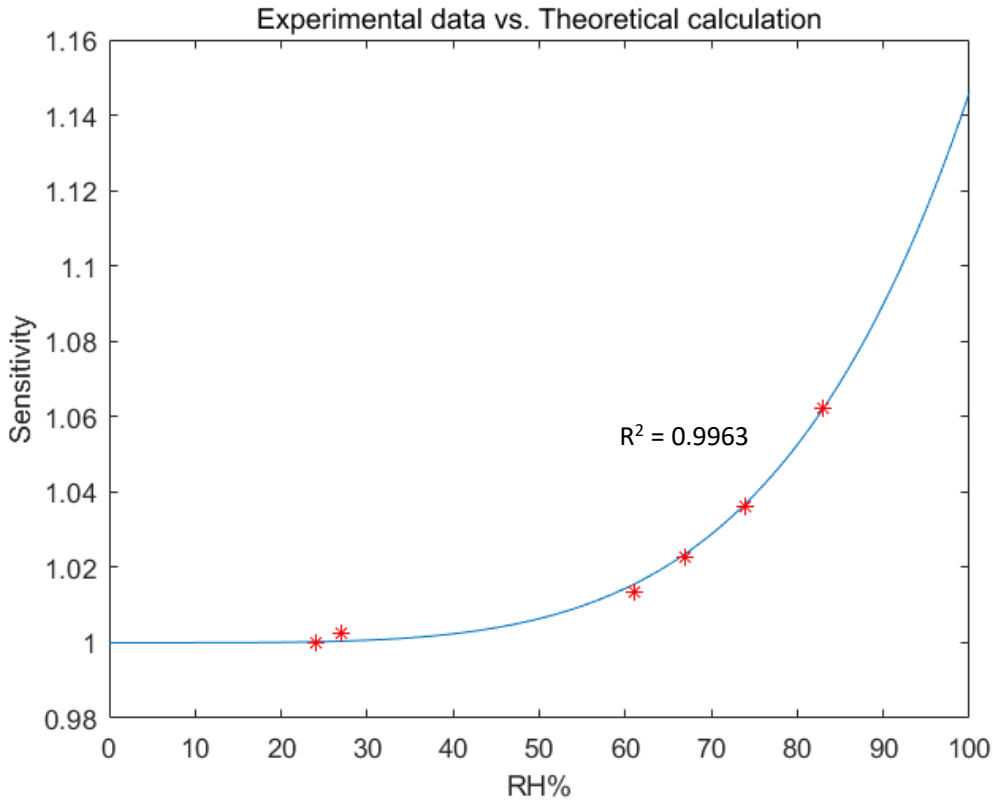

Figure 15. Fitting curve from theoretical calculation and LIG humidity sensor test result.

The previous theoretical discussion was based on the same frequency and temperature. The values of ε_1 and ε_2 used for the previous calculation is 1kHz frequency and 23°C. The relative permittivity is a complex frequency-dependent value which can relate with frequency by following equation[22]:

$$\varepsilon_r = \varepsilon'_r - i\frac{\sigma}{\omega\varepsilon_0} \tag{4.7}$$

where ε'_r is the static relative permittivity for a frequency of zero. σ is dielectric conductivity (S/m). ω is angular frequency. ε_0 is the relative permittivity of a vacuum. The capacitance of sensing material is inversely proportional to angular frequency from equation (4.7). This characteristic conforms to our experimental data.

4.2 Repeatability

In the ideal situation, the initial capacitance of the same group of LIG humidity sensors are the same, and the response curves of the capacitance vs. RH should also coincide. A group of LIG humidity sensors was made with the same procedures. During the experiment, the initial capacitance of different LIG humidity sensors may have a large difference even if they belong to the same group. Those differences are caused by each step during the procedures, such as laser cutting, transfer printing, weld the copper sheet, and so on. Those differences in initial capacitance are completely random. Figure 16 shows the 4PL fitting curve of the capacitance response to the RH of two LIG humidity sensors from the same group at 1kHz frequency. For the same group of LIG humidity sensors, the changing of capacitance for a 1%RH increase is almost the same.

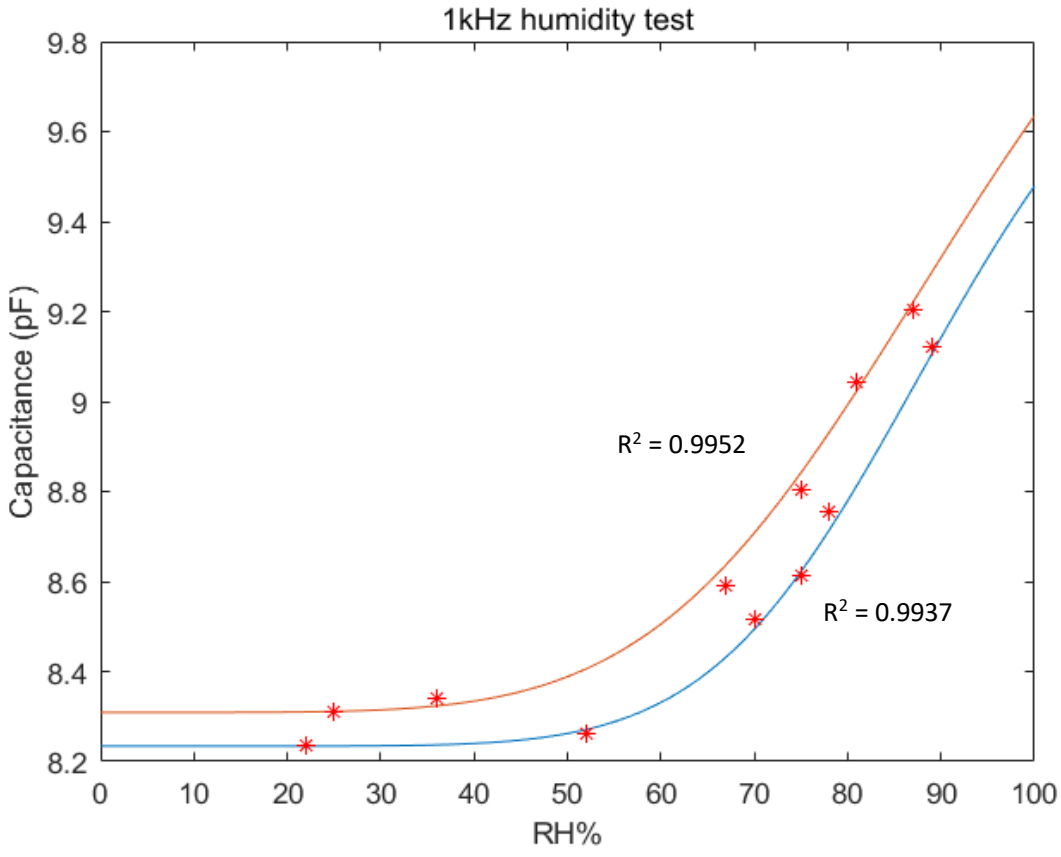

Figure 16. Humidity test of two LIG humidity sensors from the same group at 1kHz frequency.

4.3 Response and recovery time

Response and recovery time shows the speed of LIG humidity sensor response to the humidity change at a given temperature. The response time is the time that the LIG pattern absorbs water vapor from a high humidity environment. The recovery time is the time that the LIG pattern releases water vapor to the low humidity environment.[32]

During the test, the LIG humidity sensor was placed in the air with 24% relative humidity for 200 seconds, then move to another chamber with 90% relative humidity. The time of transfer humidity sensor is less than 1 second. The frequency was set at 1kHz, and temperate was 23°C.

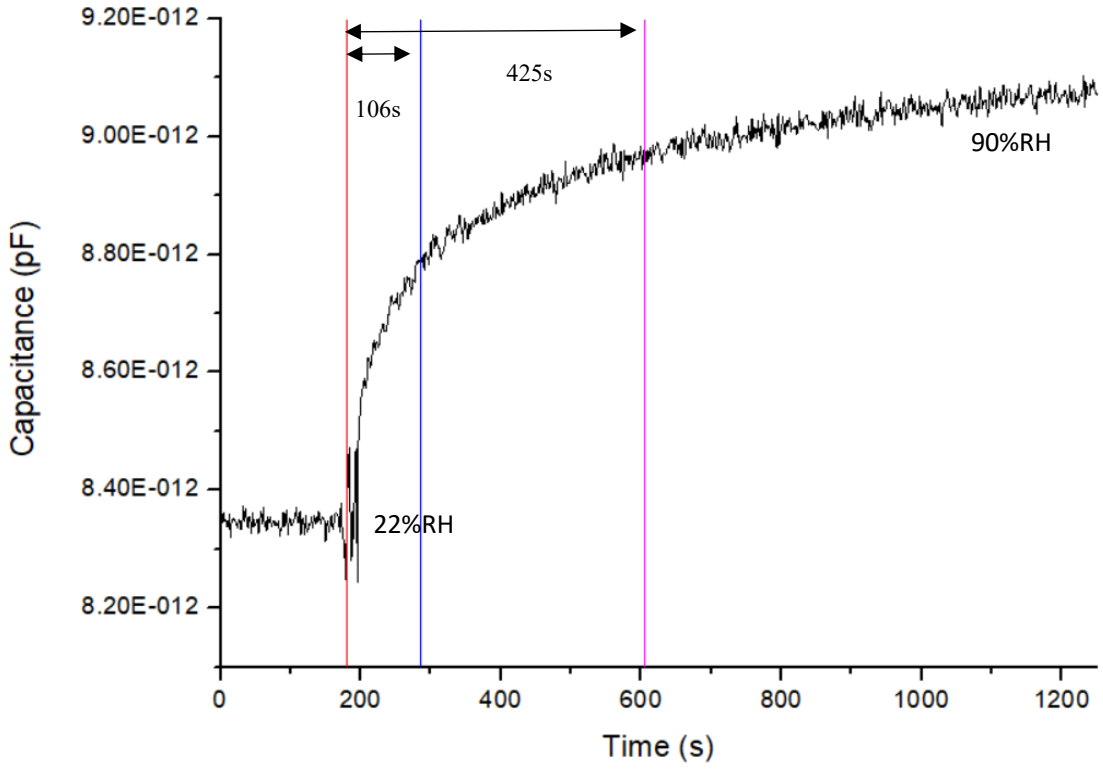

Figure 17. Response characteristics of the LIG humidity sensor toward various RH levels.

The response time is often defined by an attribute: T_{90}. This attribute indicates the time from the instant change in the variable to 90% of the final value.[56] According to the recorded data, the response time for T_{90} is ~425s. The recovery time for T_{90} is only ~13.5s. The

characteristic curves of the LIG humidity sensor are shown in Figure 17 and Figure 18.

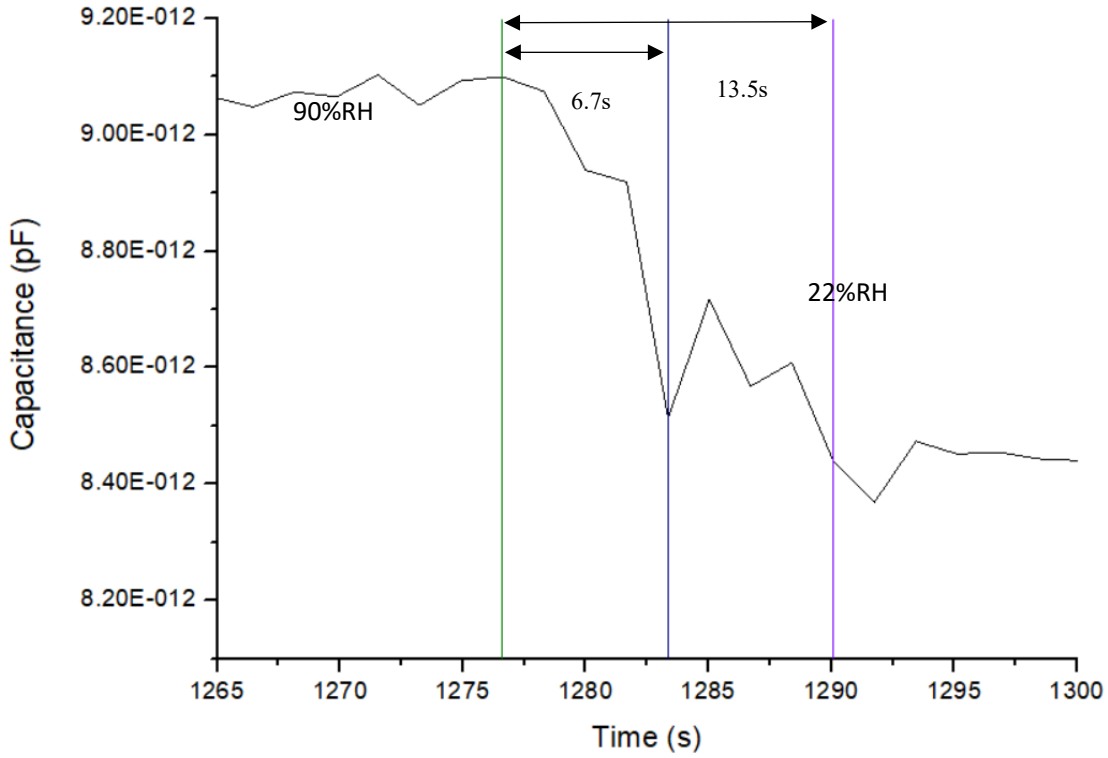

Figure 18. Recovery characteristics of the LIG humidity sensor toward various RH levels.

From the figures, it has been observed that the recovery time of the LIG humidity sensor is much shorter than response time. In general, the recovery time is usually longer than the response time for most humidity sensors.[22] During the experiment, when the LIG humidity sensor been moved from outside to the high humidity chamber. The gate of the chamber was open for about 1 second to place the sensor inside the chamber. During this 1 second, the water vapor from the humidity chamber was leaking to the surrounding air. The commercial humidity monitor was also shown a drop of humidity from 90% to 85%. Therefore, we have reason to believe the response time is not 425s, the capacitance of the LIG humidity sensor was reached 85% humidity first, and then increase along with the humidity regain after the gate was closed. Use the four parameters logistic equation from section 4.1 to calculate the capacitance at 85%RH. The capacitance of the LIG humidity sensor at 85%RH is 8.831pF. The response time

T_{90} for the LIG humidity sensor is 109s. The recovery time of the LIG humidity sensor is much better than conventional thin-film capacitive sensors made by multi-wall carbon nanotubes, silicon nanowires, macro-porous silicon, anodic aluminum oxide, graphene oxide, and so on.[19, 31, 57, 58]

	LIG	Multi-wall carbon nanotubes	Silicon nanowires	Macro-porous silicon	Graphene oxide	Anodic aluminum oxide
Response time	109s	45s	132s	20min	10.5s	188s
Recovery time	13.5s	15s	69s	unknown	41s	unknown

Table 2. Compare response time and recovery time of humidity sensors based on different materials.

LIG humidity sensor has not shown an advantage in response time compared to other thin-film capacitive humidity sensors, but it has shown a great recovery time. This character can have good usage in detection research and medical instruments. Also, the response time has shown a significant reduction with a decrease in the thickness of the sensor.[59] Therefore, the response/recovery time of the LIG humidity sensor could be further reduced. Graphene oxide and multi-wall carbon nanotubes show better response time, but these two materials require complex manufacturing processes and relatively high cost.[59]

4.4 Stability

Stability shows the ability of the humidity sensor maintains original performance in different environments.

Place the LIG humidity sensor in the humidity chamber with NaOH saturated solution (22%RH) for about 25 mins and record the real-time capacitance. During the test, the temperature was set at 23°C. The results show the short-term stability of the humidity sensor is increasing along with the increase of frequency. Short-term stability test results are depicted in Figure 19.

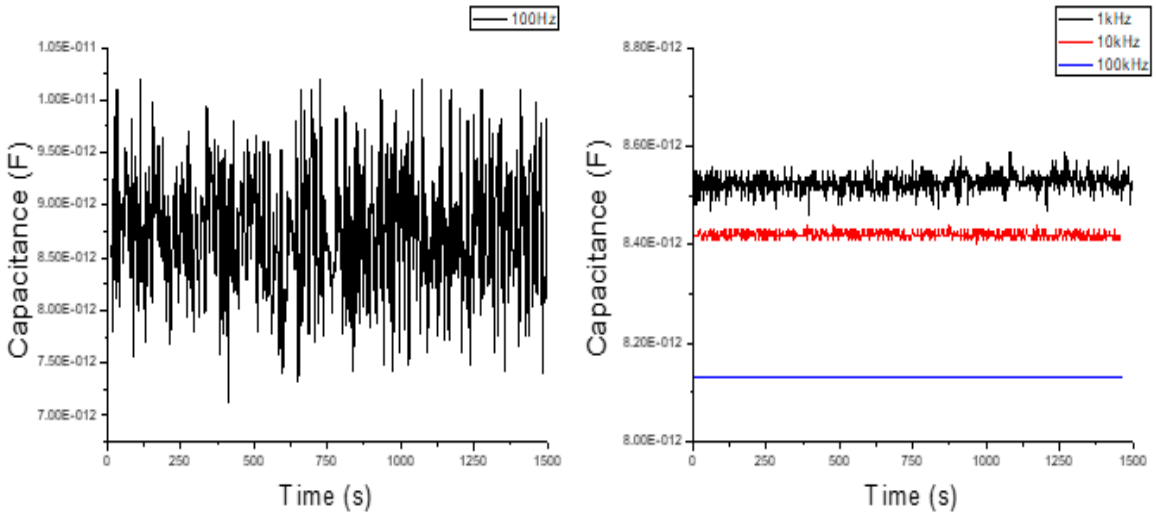

Figure 19. The left graph shows the short-term measurement capacitance of the LIG humidity sensor at 100Hz. The right graph shows the short-term measurement capacitance of the LIG humidity sensor at 1kHz, 10kHz, and 100kHz.

The test result shows the LIG humidity sensor is not stability at the frequency of 100Hz; the fluctuating value of sensitive capacitance is about ±1.6pF. The stability improves dramatically when the frequency increases up to 1kHz. The fluctuating value of sensitive capacitance is about ±0.06pF, ±0.017pF, and ±0.003pF at 1kHz, 10kHz, and 100kHz frequencies. The fluctuation of LIG humidity sensor at 100Hz, 1kHz, 10kHz, and 100kHz are 18.3%, 0.7%, 0.2%, and 0.03%. Large frequency (over 1kHz) has great stability in the short-term.

The influence of different gases is also tested. Inject 1000ppm of NH_3, NO_2, ethanol, and methanol into the humidity chamber by using a pipette and needle tube. The result shows the

capacitance of the LIG humidity sensor changed less than 1% when 1000ppm NO_2 was put into the chamber. The capacitance of the LIG humidity sensor changed less than 0.1% when the other three gases were put into the chamber. The low capacitance change response to those gases shows the effect of those gases to the LIG humidity sensor is neglectable.

Conclusion and future works

5.1 Conclusion

A humidity sensor is an important tool in the environment and health monitoring. With technology developing, humanities are paying more attention to their health condition and improve their quality of life. Therefore, micro-motion and wearable types of humidity sensors conform to the time.

After a year of study, I finish the design, prepare the sample, experiment setup, and result test. This research is based on new material——Laser-induced Graphene, and its great electric properties to design and test a flexible humidity sensor. Base on the test result, the sensitivity, repeatability, response/recovery time, and short-term stability of the LIG humidity sensor are studied during the experiment. The sensitivity of our LIG humidity sensor is relatively low compared to other capacitive type humidity.

A comprehensive comparison between the LIG capacitive humidity sensor and other capacitive humidity sensors shows some benefit of the LIG humidity sensor. The LIG material was manufactured from PI film, which is also the humidity sensing material. The sensitivity of the LIG humidity sensor is 15% at 1kHz, which is larger than the PI-based humidity sensor (~10% sensitivity)[39]. However, it is relatively low compared to other thin-film capacitive humidity sensors. For example, ordered macro-porous silicon-based capacitive humidity sensor exhibit over 100% sensitivity, but the response time of this material is over 20mins.[58] Metal oxide materials are often used humidity sensing material for capacitive humidity sensor. An anodic aluminum oxide-based humidity sensor exhibit sensitivity for over 600%, but the

response curve of the capacitance and relative humidity is non-linear. The capacitance versus RH is almost a straight line until RH reaches about 80%, then the capacitance increasing dramatically. The nonlinearity can greatly affect the measurement range and accuracy of the anodic aluminum oxide-based humidity sensor.[16] Other than performances, the fabrication process of LIG is easier than other materials. A comprehensive comparison of performance and fabrication process between LIG-based capacitive humidity and others are shown in Table 3.

	LIG	Multi-wall carbon nanotubes	Silicon nanowires	Macro-porous silicon	Graphene oxide	Anodic aluminum oxide
Sensitivity	15%	3000%	78.8%	297.5%	37800%	600%
Linearity	Non-linear	Non-linear	Linear	linear	Non-linear	Non-linear
Response/recovery time	109s/13.5s	45s/15s	132s/69s	20min	10.5s/41s	188s
Fabrication process	Laser-induced on PI film	Chemical vapor deposition (CVD)67]	Chemical etching procedure	Electrochemical etching of (1 0 0)-oriented n-type Si in hydrofluoric acid (HF) with Backside illumination	Chemical Synthesis[68]	Complementary metal oxide semiconductor-Micro electro mechanical system (CMOS-MEMS) technology[69]

Table 3. A comprehensive comparison of performance and fabrication process between LIG-based capacitive humidity and other material based capacitive humidity sensors.[67-69]

Overall, the LIG capacitive humidity sensor has shown considerable sensitivity, and the experimental result highly consistent with the theoretical calculation. The result also shows an ultrafast recovery time of the LIG humidity sensor. LIG humidity sensor also shows great repeatability and short-term stability, especially the minimized capacitance response to other chemistry gases, which can eliminate the error corresponding to different air composition. In conclusion, LIG has a great humidity sensing material to manufacture high performance, low-cost and easy process capacitive humidity sensor.

5.2 Problems and future works

The humidity sensor has been studied and developed for many years. There are many commercial products on the market. The measurement accuracy and response/recovery time are always a problem. The best commercial humidity sensor has the accuracy of ±1%RH, which is caused by its poor linearity.[19]

There is still a big room for improvement for LIG-based humidity sensor can be studied in the future:

1 Improve transfer print technology.

The transfer print has a large effect on the LIG structure. LIG has a porous structure and fragile surface, direct contact with other rough surfaces could cause permanent damage to the contact part. During the transfer print process, the PI film was separated from LIG by deformation in a short time. This process can cause inevitable damage to the porous structure of LIG. The capacitance value of the LIG-based humidity sensor decreased 5% after the transfer print process. Unfortunately, this is the only stability way we have to transfer the LIG pattern onto a flexible silicon substrate.

2 Improve the way to measure response time.

During the experiment of response time, water vapor inside the humidity chamber leak to the outside environment when the gate was open. The relative humidity drop from 90% to 85% was observed with a commercial humidity sensor. The relative humidity then regains from the saturate salt solution until RH reaches 90%. The RH regain very slow; this affects our response

time measurement. Therefore, we need to re-design a chamber gate in order to place our sample inside without a large opening.

3 Measure long-term stability.

Due to the time consuming and equipment limit, I am unable to measure the long-term stability of the LIG humidity sensor. Long-term stability is an important property to determine whether the sensor is able to maintain work for a long period. It does affect not only the service life of the humidity sensor but also the accuracy of the humidity sensor for long-term usage.[60, 61] The future plan is to measure the same LIG humidity sensor every week for at least three months.

4 Study the stretch affect the LIG humidity sensor.

The LIG humidity sensor was transferred onto a flexible substrate to make a wearable sensor. Therefore the bend and stretch effect the capacitance and all the performance parameters (sensitivity, repeatability, stability, and response/recovery time) is another unfinished. Also, it is very important to demonstrate some mechanic properties, such as maximum stretch length. I plan to use the motion stage and source meter to be an experiment plate and measuring apparatus.

5 Improve the sensitivity of the LIG humidity sensor.

From the previous section, the sensitivity of the LIG humidity sensor is not very high. The sensitivity of the LIG humidity sensor is ~15% at 1kHz frequency.

Increase the sensitivity of the LIG humidity sensor can reduce the effect of measurement error, which helps improve the accuracy of the sensor.[62] The sensitivity is in direct proportion to the volume fraction of water vapor by sensing material. The LIG is a hydrophobic material that greatly reduced the water absorption of LIG.[63] UV/ozone treatment can increase hydrophilic of the LIG surface, which may potentially increase the sensitivity of the LIG humidity sensor.[64]

6 Study the relationship between dielectric loss and relative humidity

In recent experiments, we discovered another electric parameter that response to the relative humidity changes. Dielectric loss shows a great response/recovery time response to the relative humidity changes. Figure 20 shows a comparison result of dielectric loss and capacitance response to RH of LIG humidity sensor at 1kHz frequency during the same test.

The result shows the response time of dielectric loss is approximately 20s, and the recovery time is 13s. This response/recovery speed is better than all commercial humidity sensor products without preheating. This result has also shown a disadvantage of dielectric loss response, which is the fluctuation up to ±15%, while the fluctuation of capacitance is ±15%.

The fluctuation could be reduced by increasing the frequency, but it may also reduce its sensitivity. We need to do further investigation and experiments on that.

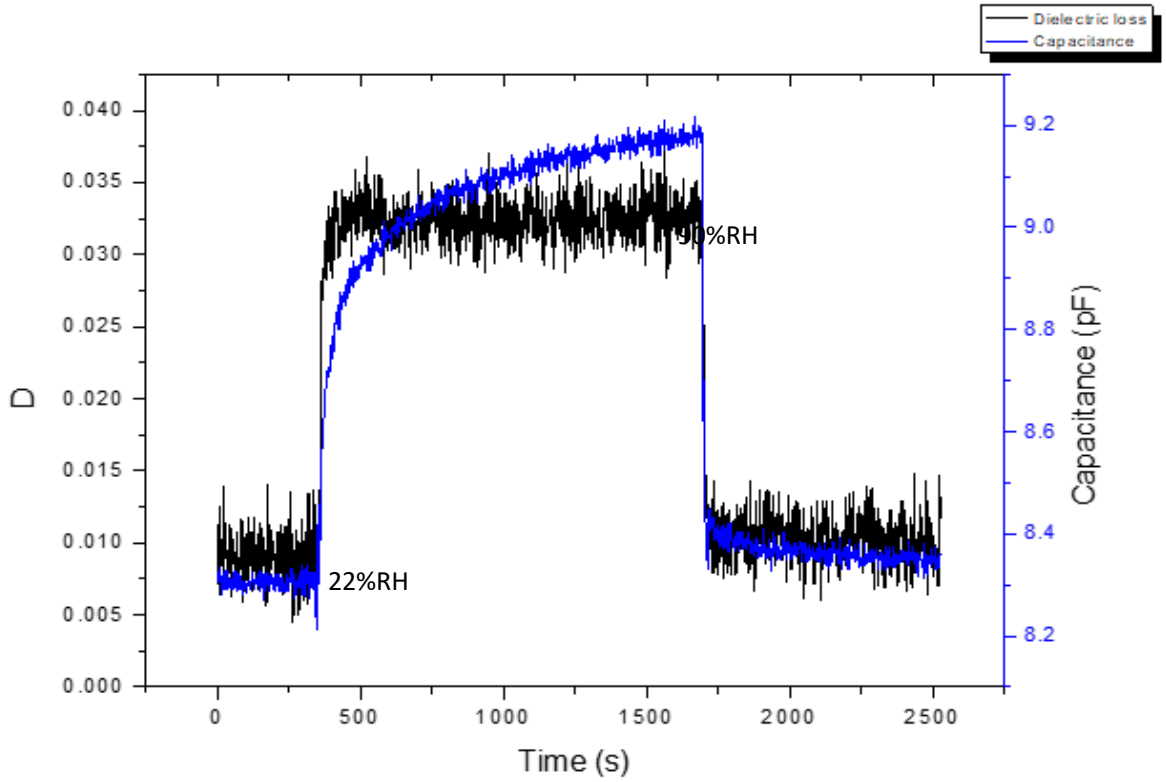

Figure 20. Result of dielectric loss and capacitance of the LIG humidity sensor response to the relative humidity at 1kHz frequency.

The dielectric loss also shows high sensitivity and highly linear response curves versus relative humidity levels. The resulting curve is shown in Figure 21. The sensitivity of the dielectric loss characteristic is ~200%. The transformed response curves of dielectric loss sensitivity vs. RH of LIG-based capacitive sensor also show great two-stage linearity. The sensitivity of the dielectric loss characteristic at low RH range is 0.165/%RH, then the sensitivity increase to 5.191/%RH. The turning point is at approximately 55%RH. There was no research studied on the dielectric loss characteristic direct response to RH. Therefore this is a new research direction that could lead to a new type of humidity sensor.

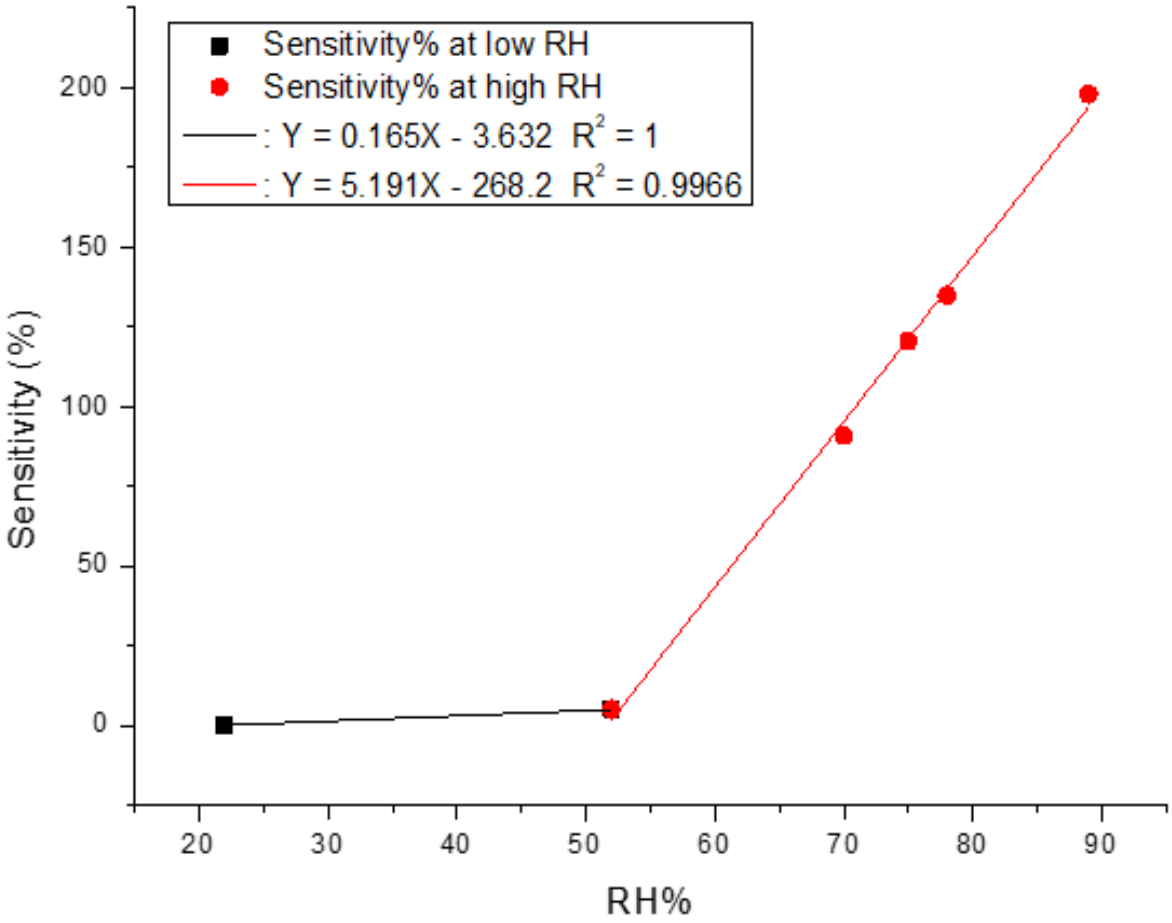

Figure 21. The sensitivity vs. RH of the dielectric loss characteristic of the LIG humidity sensor at 1kHz.

In a word, study LIG-based capacitive humidity sensor is a systematized project. It includes design, manufacture, and test so on. There is room for improvement for every step that requires further and deeper research.

References

[1] Sensor. (2019, October 28). Retrieved from https://en.wikipedia.org/wiki/Sensor.

[2] Cai, H., Li, X., Chen, Z., & Kong, L. (2013). Fast identification of multiple indoor constant contaminant sources by ideal sensors: a theoretical model and numerical validation. Indoor and Built Environment, 22(6), 897-909.

[3] Lorek, A., & Koncz, A. (2010). Development of a gas flow independent coulometric trace humidity sensor for aerospace and industry. Deutsches Zentrum für Luft-und Raumfahrt, 2, 1.

[4] Relative Humidity in Production and Process Environments. (n.d.). Retrieved from https://www.engineeringtoolbox.com/relative-humidity-production-process-d_511.html.

[5] Lowen, A. C., Mubareka, S., Steel, J., & Palese, P. (2007). Influenza virus transmission is dependent on relative humidity and temperature. PLoS pathogens, 3(10), e151.

[6] Srbinovska, M., Gavrovski, C., Dimcev, V., Krkoleva, A., & Borozan, V. (2015). Environmental parameters monitoring in precision agriculture using wireless sensor networks. Journal of cleaner production, 88, 297-307.

[7] Boyer, J. S., & Knipling, E. B. (1965). Isopiestic technique for measuring leaf water potentials with a thermocouple psychrometer. Proceedings of the National Academy of Sciences of the United States of America, 54(4), 1044.

[8] Kulwicki, B. M. (1991). Humidity sensors. Journal of the American Ceramic Society, 74(4), 697-708.

[9] Yamazoe, N., & Shimizu, Y. (1986). Humidity sensors: principles and applications. Sensors and Actuators, 10(3-4), 379-398.

[10] Moisture and Humidity Control Solution in Pharmaceutical Industry: Bry-Air. (n.d.).

Retrieved from https://www.bryair.com/industries-applications/applications-of-dehumidifiers-and-dryers/production-and-processing/pharmaceutical-

[11] The Capacitive Humidity Sensor. (n.d.). Retrieved from https://www.rotronic.com/en-us/humidity_measurement-feuchtemessung-mesure_de_l_humidite/capacitive-sensors-technical-notes-mr.

[12] Relative permittivity. (2019, October 17). Retrieved from https://en.wikipedia.org/wiki/Relative_permittivity.

[13] Nasreen, S., Treich, G. M., Baczkowski, M. L., Mannodi‐Kanakkithodi, A. K., Cao, Y., Ramprasad, R., & Sotzing, G. (2000). Polymer dielectrics for capacitor application. Kirk‐Othmer Encyclopedia of Chemical Technology, 1-29.

[14] Lee, S. P. (2017). Electrodes for semiconductor gas sensors. Sensors, 17(4), 683.

[15] Schubert, P. J., & Nevin, J. H. (1985). A polyimide-based capacitive humidity sensor. IEEE transactions on electron devices, 32(7), 1220-1223.

[16] Kim, Y., Jung, B., Lee, H., Kim, H., Lee, K., & Park, H. (2009). Capacitive humidity sensor design based on anodic aluminum oxide. Sensors and Actuators B: Chemical, 141(2), 441-446.

[17] Zhang, D., Sun, Y. E., Li, P., & Zhang, Y. (2016). Facile fabrication of MoS2-modified SnO2 hybrid nanocomposite for ultrasensitive humidity sensing. ACS applied materials & interfaces, 8(22), 14142-14149.

[18] Ahmad, W. R. W., Mamat, M. H., Zoolfakar, A. S., Khusaimi, Z., & Rusop, M. (2016, December). A review on hematite α-Fe 2 O 3 focusing on nanostructures, synthesis methods and applications. In 2016 IEEE Student Conference on Research and Development (SCOReD)

(pp. 1-6). IEEE.

[19] Chen, W. P., Zhao, Z. G., Liu, X. W., Zhang, Z. X., & Suo, C. G. (2009). A capacitive humidity sensor based on multi-wall carbon nanotubes (MWCNTs). Sensors, 9(9), 7431-7444.

[20] Anusha. (2017, December 25). Humidity Sensor - Types and Working Principle. Retrieved from https://www.electronicshub.org/humidity-sensor-types-working-principle/.

[21] Farahani, H., Wagiran, R., & Hamidon, M. N. (2014). Humidity sensors principle, mechanism, and fabrication technologies: a comprehensive review. Sensors, 14(5), 7881-7939.

[22] Tripathy, A., Pramanik, S., Manna, A., Bhuyan, S., Azrin Shah, N., Radzi, Z., & Abu Osman, N. (2016). Design and development for capacitive humidity sensor applications of lead-free Ca, Mg, Fe, Ti-oxides-based electro-ceramics with improved sensing properties via physisorption. Sensors, 16(7), 1135.

[23] Lin, J., Peng, Z., Liu, Y., Ruiz-Zepeda, F., Ye, R., Samuel, E. L., ... & Tour, J. M. (2014). Laser-induced porous graphene films from commercial polymers. Nature communications, 5, 5714.

[24] Ye, R., James, D. K., & Tour, J. M. (2018). Laser-induced graphene. Accounts of chemical research, 51(7), 1609-1620.

[25] Li, D., & Kaner, R. B. (2008). Graphene-based materials. Science, 320(5880), 1170-1171.

[26] Graphene. (2019, November 1). Retrieved from https://en.wikipedia.org/wiki/Graphene.

[27] Aron, J. (2015, May 27). Spacecraft built from graphene could run on nothing but sunlight. Retrieved from https://www.newscientist.com/article/mg22630235-400-spacecraft-built-from-graphene-could-run-on-nothing-but-sunlight/.

[28] Huang, Y., Liang, J., & Chen, Y. (2012). An overview of the applications of graphene -

based materials in supercapacitors. Small, 8(12), 1805-1834.

[29] Sanz, J. (2010). The influence of morphology and long range interactions in the electronic properties of graphene.

[30] Wang, C., Vinodgopal, K., & Dai, G. P. (2018). Large-Area Synthesis and Growth Mechanism of Graphene by Chemical Vapor Deposition. In Chemical Vapor Deposition for Nanotechnology. IntechOpen.

[31] Zhang, Y. I., Zhang, L., & Zhou, C. (2013). Review of chemical vapor deposition of graphene and related applications. Accounts of chemical research, 46(10), 2329-2339.

[32] Bi, H., Yin, K., Xie, X., Ji, J., Wan, S., Sun, L., ... & Dresselhaus, M. S. (2013). Ultrahigh humidity sensitivity of graphene oxide. Scientific reports, 3, 2714.

[33] Chen, M. C., Hsu, C. L., & Hsueh, T. J. (2014). Fabrication of humidity sensor based on bilayer graphene. IEEE Electron Device Letters, 35(5), 590-592.

[34] Wang, J., Wang, X. H., & Wang, X. D. (2005). Study on dielectric properties of humidity sensing nanometer materials. Sensors and Actuators B: Chemical, 108(1-2), 445-449.

[35] Oberländer, J., Jildeh, Z., Kirchner, P., Wendeler, L., Bromm, A., Iken, H., ... & Schöning, M. (2015). Study of interdigitated electrode arrays using experiments and finite element models for the evaluation of sterilization processes. Sensors, 15(10), 26115-26127.

[36] Clifford, Paul. “Calculating Electrolytic Conductivity Sensor Cell Constant for Microfabricated Planar Interdigitated Electrode Array, Conductivity Cell Constant.” Find Controllers for Instrumentation and Automation at the Mosaic Industries Site, Mosaic Industries, Inc., http://www.mosaic-industries.com/embedded-systems/instrumentation/conductivity-meter/microfabricated-planar-interdigitated-electrodes-

cell-constant.

[37] Archimedean spiral. (2019, October 17). Retrieved from https://en.wikipedia.org/wiki/Archimedean_spiral.

[38] Thomson, G. W. (1946). The Antoine equation for vapor-pressure data. Chemical reviews, 38(1), 1-39.

[39] Lei Gu. The design of a capacitive relative humidity sensor with COMS process. [Thesis for the academic degree of Master of Engineering]. The department of Electronic Engineering Southeast University, February 2004

[40] Lawrence, M. G. (2005). The relationship between relative humidity and the dewpoint temperature in moist air: A simple conversion and applications. Bulletin of the American Meteorological Society, 86(2), 225-234.

[41] Childres, I., Jauregui, L. A., Park, W., Cao, H., & Chen, Y. P. (2013). Raman spectroscopy of graphene and related materials. New developments in photon and materials research, 1.

[42] Pimenta, M. A., Dresselhaus, G., Dresselhaus, M. S., Cancado, L. G., Jorio, A., & Saito, R. (2007). Studying disorder in graphite-based systems by Raman spectroscopy. Physical chemistry chemical physics, 9(11), 1276-1290.

[43] Rittersma, Z. M., Splinter, A., Bödecker, A., & Benecke, W. (2000). A novel surface-micromachined capacitive porous silicon humidity sensor. Sensors and Actuators B: Chemical, 68(1-3), 210-217.

[44] Gallagher, A. J., Ní Annaidh, A., & Bruyère, K. (2012). Dynamic tensile properties of human skin. In IRCOBI Conference 2012, 12-14 September 2012, Dublin (Ireland). International Research Council on the Biomechanics of Injury.

[45] Johnston, I. D., McCluskey, D. K., Tan, C. K. L., & Tracey, M. C. (2014). Mechanical characterization of bulk Sylgard 184 for microfluidics and microengineering. Journal of Micromechanics and Microengineering, 24(3), 035017.

[46] Mann, S., Kumar, R., & Jindal, V. K. (2017). Negative thermal expansion of pure and doped graphene. RSC Advances, 7(36), 22378-22387.

[47] Liu, F., Liu, Z., Gao, S., You, Q., Zou, L., Chen, J., ... & Liu, X. (2018). Polyimide film with low thermal expansion and high transparency by self-enhancement of polyimide/SiC nanofibers net. RSC advances, 8(34), 19034-19040.

[48] Quincot, G., Azenha, M., Barros, J., & Faria, R. (2011). Use of salt solutions for assuring constant relative humidity conditions in contained environments. Fundação para a Ciência e a Tecnologia.

[49] Bowler, M. G., Bowler, D. R., & Bowler, M. W. (2017). Raoult's law revisited: accurately predicting equilibrium relative humidity points for humidity control experiments. Journal of applied crystallography, 50(2), 631-638.

[50] Saturated Salt Solutions and Air Humidity. (n.d.). Retrieved from https://www.engineeringtoolbox.com/salt-humidity-d_1887.html.

[51] O'Connell, M. A., Belanger, B. A., & Haaland, P. D. (1993). Calibration and assay development using the four-parameter logistic model. Chemometrics and Intelligent Laboratory Systems, 20(2), 97-114.

[52] VØlund, A. (1978). Application of the four-parameter logistic model to bioassay: comparison with slope ratio and parallel line models. Biometrics, 357-365.

[53] Nelson, S. O. (2004). Useful relationships between dielectric properties and bulk densities

of granular and powdered materials. Am. Inst. Chem. Eng. Ann., 136-140.

[54] Shibata, H., Ito, M., Asakursa, M., & Watanabe, K. (1996). A digital hygrometer using a polyimide film relative humidity sensor. IEEE Transactions on Instrumentation and Measurement, 45(2), 564-569.

[55] Patel, K., Neha, & Tyagi, P. K. (2016, May). Effective relative permittivity and characteristic impedance of graphene loaded microstrip line by scalar S-parameters. In AIP Conference Proceedings (Vol. 1728, No. 1, p. 020617). AIP Publishing.

[56] Response time in humidity measurement. (n.d.). Retrieved from https://www.vaisala.com/sites/default/files/documents/Response-time-in-humidity-measurement-Technical-Note-B211803EN.pdf.

[57] Wang, Y., Park, S., Yeow, J. T., Langner, A., & Müller, F. (2010). A capacitive humidity sensor based on ordered macroporous silicon with thin film surface coating. Sensors and Actuators B: Chemical, 149(1), 136-142.

[58] Chen, X., Zhang, J., Wang, Z., Yan, Q., & Hui, S. (2011). Humidity sensing behavior of silicon nanowires with hexamethyldisilazane modification. Sensors and Actuators B: Chemical, 156(2), 631-636.

[59] Steele, J. J., Taschuk, M. T., & Brett, M. J. (2009). Response time of nanostructured relative humidity sensors. Sensors and Actuators B: Chemical, 140(2), 610-615.

[60] Jankovec, M., Galliano, F., Annigoni, E., Li, H. Y., Sculati-Meillaud, F., Ballif, C., ... & Topič, M. (2000). Long term stability of humidity sensors, laminated in EVA encapsulant. MIDEM, 2(0), 1.

[61] Matsuguchi, M., Kuroiwa, T., Miyagishi, T., Suzuki, S., Ogura, T., & Sakai, Y. (1998).

Stability and reliability of capacitive-type relative humidity sensors using crosslinked polyimide films. Sensors and actuators B: Chemical, 52(1-2), 53-57.

[62] Antikainen, V., & Paukkunen, A. (1994). Studies on improving humidity measurements in radiosondes. In Proc. WMO Tech. Conf.

[63] Ahmad, D., van den Boogaert, I., Miller, J., Presswell, R., & Jouhara, H. (2018). Hydrophilic and hydrophobic materials and their applications. Energy Sources, Part A: Recovery, Utilization, and Environmental Effects, 40(22), 2686-2725.

[64] Oláh, A., Hillborg, H., & Vancso, G. J. (2005). Hydrophobic recovery of UV/ozone treated poly (dimethylsiloxane): adhesion studies by contact mechanics and mechanism of surface modification. Applied Surface Science, 239(3-4), 410-423.

[65] Hannay, J. H. (1983). The Clausius-Mossotti equation: an alternative derivation. European Journal of Physics, 4(3), 141.

[66] Gillespie, L. J. (1930). The Gibbs-Dalton law of partial pressures. Physical Review, 36(1), 121.

[67] Rigueur, J. L. (2012). Multiwalled carbon nanotube films: fabrication techniques and applications. Vanderbilt University.

[68] Adetayo, A., & Runsewe, D. (2019). Synthesis and Fabrication of Graphene and Graphene Oxide: A Review. Open Journal of Composite Materials, 9(02), 207.

[69] Dai, C. L. (2007). A capacitive humidity sensor integrated with micro heater and ring oscillator circuit fabricated by CMOS–MEMS technique. Sensors and Actuators B: Chemical, 122(2), 375-380.